

1 **Modeling productivity of silver birch (*Betula pendula* Roth.) combining**
2 **phytogenic and geocentric approaches in northwestern Europe**

3

4 Lorna Zeoli^a, Tom De Mil^a, Aurélien Forler^a, Mathilde Pau^a, Nicolas Latte^a, Hugues
5 Claessens^a, Gauthier Ligot^a

6 ^a University of Liège, Gembloux Agro-Bio Tech, Terra-Forest is life, 5030 Gembloux, Belgium

7 **Corresponding author:** Lorna.Zeoli@uliege.be

8 **E-mail addresses of the other authors:** tom.demil@uliege.be,
9 aurelien.forler@agroparistech.fr, mathilde.pau@uliege.be, nicolas.latte@uliege.be,
10 hugues.claessens@uliege.be, gligot@uliege.be.

11 **Abstract**

12 The current climate emergency and its associated impacts on forest ecosystems are leading
13 forest owners and managers to consider a broader diversity of species to enhance forest
14 resilience. In this context, there is a growing interest in lesser-used timber species, such as silver
15 birch, a promising candidate for forest diversification in Western Europe. Estimates of site
16 productivity are essential to guide forest management decisions, but have not yet been
17 accurately determined for silver birch in northwestern Europe. This study pursues two main
18 goals: (a) providing dominant height growth curves for birch in southern Belgium; (b)
19 identifying the key biophysical factors affecting the productivity of silver birch within the study
20 area.

21 In this study, we tested and compared 16 growth models on a stem analysis dataset gathering
22 the past height growth of 68 birch trees from 40 stands. The Duplat and Tran-Ha I model best
23 predicted the dominant height growth. Using this model, the site index (SI) was estimated for
24 103 stands distributed throughout the study area and its variation was modeled in response to
25 biophysical variables (climatic, edaphic and topographic). The best selected model (R^2
26 $_{adj}=0.50$) revealed a positive effect of mean annual temperature on the SI, although limited
27 when maximal soil water content was low. This model was ultimately used to map the spatial
28 variation in birch yield potential in the study area, highlighting the ecological conditions under
29 which birch silviculture could be promoted.

30 **Keywords**

31 *Betula pendula* – Silver birch – Site index – Height growth – Soil water content – Mean annual
32 temperature

33 **1 Introduction**

34 Forests provide a wide range of essential services contributing to human well-being worldwide
35 (Brockhoff et al., 2017). However, the significant increase in natural disturbances poses a
36 serious threat to the provisioning of forest ecosystem services (Patacca et al., 2023; Wolf and
37 Paul-Limoges, 2023). Over the last decades, European forests have experienced an increase in
38 extreme events related to climate change (Büntgen et al., 2021). As a result, increased mortality
39 has been observed for all major tree species (George et al., 2022). Norway spruce (*Picea abies*),
40 one of the most important economic species in Europe, has greatly suffered from the extreme
41 drought of 2018, whose conditions favored a bark beetle outbreak, leading to several million
42 hectares of damaged forests (Arthur et al., 2024; Hlásny et al., 2021). European beech (*Fagus*
43 *sylvatica*), another major timber tree species, has also demonstrated high climate sensitivity,
44 with significant growth declines ranging from -20% to -90% depending on the region
45 considered, to be expected by 2090 (Martinez del Castillo et al., 2022). Mortality episodes have
46 also been observed in species previously noted as drought-tolerant, including pedunculate and
47 sessile oaks (*Quercus robur*, *Quercus petraea*), as well as Scots pine (*Pinus sylvestris*; Schuldt
48 et al., 2020). This alarming context forces us to deeply reconsider the way forests are managed
49 (Bolte et al., 2009; Millar et al., 2007).

50 One solution consists of enhancing forest resilience by promoting forest diversification through
51 the integration of species presumed to be more tolerant to future climatic conditions (Bolte et
52 al., 2009; Messier et al., 2022). Forest diversification can be ensured by selecting non-native
53 species or provenances better adapted to the future climatic conditions (Williams and
54 Dumroese, 2013). However, the introduction of non-native species, although drought-tolerant,
55 entails major risks for native biodiversity as this might lead to habitat losses and introduction
56 of invasive species (Aurore et al., 2024; Dimitrova et al., 2022; Felton et al., 2016; Mueller and
57 Hellmann, 2008). Alternatively, the possibility of enriching forest stands with abundant but

58 lesser used timber species, e.g., Norway maple (*Acer platanoides*), European hornbeam
59 (*Carpinus betulus*), little leaved lime (*Tilia cordata*), silver birch (*Betula pendula*), is
60 increasingly being considered (Koch et al., 2022; Walentowski et al., 2017) even though their
61 vulnerability to climate change remains to be clarified (Fuchs et al., 2021; Hemery et al., 2010;
62 Kunz et al., 2018; Latte et al., 2020; Leuschner et al., 2024; Matisons et al., 2022). Among
63 those indigenous species, silver birch (*Betula pendula* Roth.) seems to be a promising candidate
64 (Biber et al., 2020; Dubois et al., 2020).

65 Silver birch is a light-demanding pioneer species distributed throughout Eurasia, which
66 represents the widest distribution range of all European broadleaved tree species (Ellenberg,
67 1996). This exceptionally large ecological range is explained by the broad climatic tolerance
68 and sustained growth on various soil conditions, even on constraining sites (Atkinson, 1992).
69 Birch colonizes disturbed environments and can contribute to the rapid restoration of wood
70 production, highlighting the importance of early successional stages in maintaining forest
71 ecosystem resilience (Bormann et al., 2015; Swanson et al., 2010). As a nurse species, birch
72 creates favorable conditions for the establishment of other species (Stark et al., 2015). It
73 provides light in the understory and improves soil fertility, porosity and water infiltration,
74 promoting the development of mixed forests (Jonczak et al., 2020; Perala and Alm, 1990).
75 Apart from the Baltics and Finland, silver birch has received little attention for commercial
76 purposes (Dubois et al., 2020; Hynynen et al., 2010; Lee et al., 2024). However, the physical
77 and mechanical properties of birch timber make it as valuable as beech, a species of significant
78 economic importance (Luostarinen and Verkasalo, 2000). Birch species are gaining in
79 popularity in Western Europe where the possibility of producing large-sized logs with adapted
80 and dynamic silvicultural practices has recently been assessed (Dubois et al., 2021). The short
81 rotation associated with birch silviculture (50 years; Dubois et al., 2021) is a significant
82 advantage in the context of climate change, as trees are exposed to extreme climatic events for

83 a shorter period of time (Lindner *et al.*, 2000; Spittlehouse and Stewart, 2003). As birch has
84 only recently gained the interest of foresters, key information for its management, especially
85 regarding its productivity potential, is still lacking.

86 Site productivity refers to the quantitative estimation of a site-specific capacity to produce plant
87 biomass (Skovsgaard and Vanclay, 2008). This estimation remains crucial for guiding forest
88 management decisions, helping forest owners and managers in species selection (i.e., species-
89 site suitability), designing optimal silvicultural strategies, predicting timber yield, and assessing
90 carbon sequestration potential. Site productivity can be estimated through two approaches
91 (Skovsgaard and Vanclay, 2008): phytocentric and geocentric. For even-aged stands, the
92 phytocentric approach is usually applied to estimate the site index (SI), i.e., the dominant height
93 reached by a forest stand at a reference age (Skovsgaard and Vanclay, 2008). As the height
94 growth of dominant tree is known to be less affected by stand density than its diameter growth,
95 SI mainly depends on site conditions (Spurr and Barnes, 1973). Dominant height growth curves,
96 linking height and age of dominant trees, have usually been modeled using nonlinear
97 relationships. The resulting models have notably been used to predict the dominant height at a
98 given age and, therefore, to estimate phytocentric SI.

99 However, in some situations (e.g. unknown forest stand age, non-forested area, juvenile stand),
100 SI cannot be assessed using phytocentric methods and can be estimated from other site
101 characteristics using a geocentric approach (Skovsgaard and Vanclay, 2008). This approach is
102 based on the empirical relationship between site productivity and biophysical factors (climate,
103 soil and topography). This method can take into account the non-stationarity of forest
104 productivity over time, which is crucial in the context of climate change (Bontemps *et al.*,
105 2009). The geocentric approach have been used to predict future trends in height growth (Albert
106 and Schmidt, 2010; Brandl *et al.*, 2018; Pau *et al.*, 2022) and to better understand the ecological
107 niche constraints of species (Seynave *et al.*, 2008). As spatial biophysical data are often easily

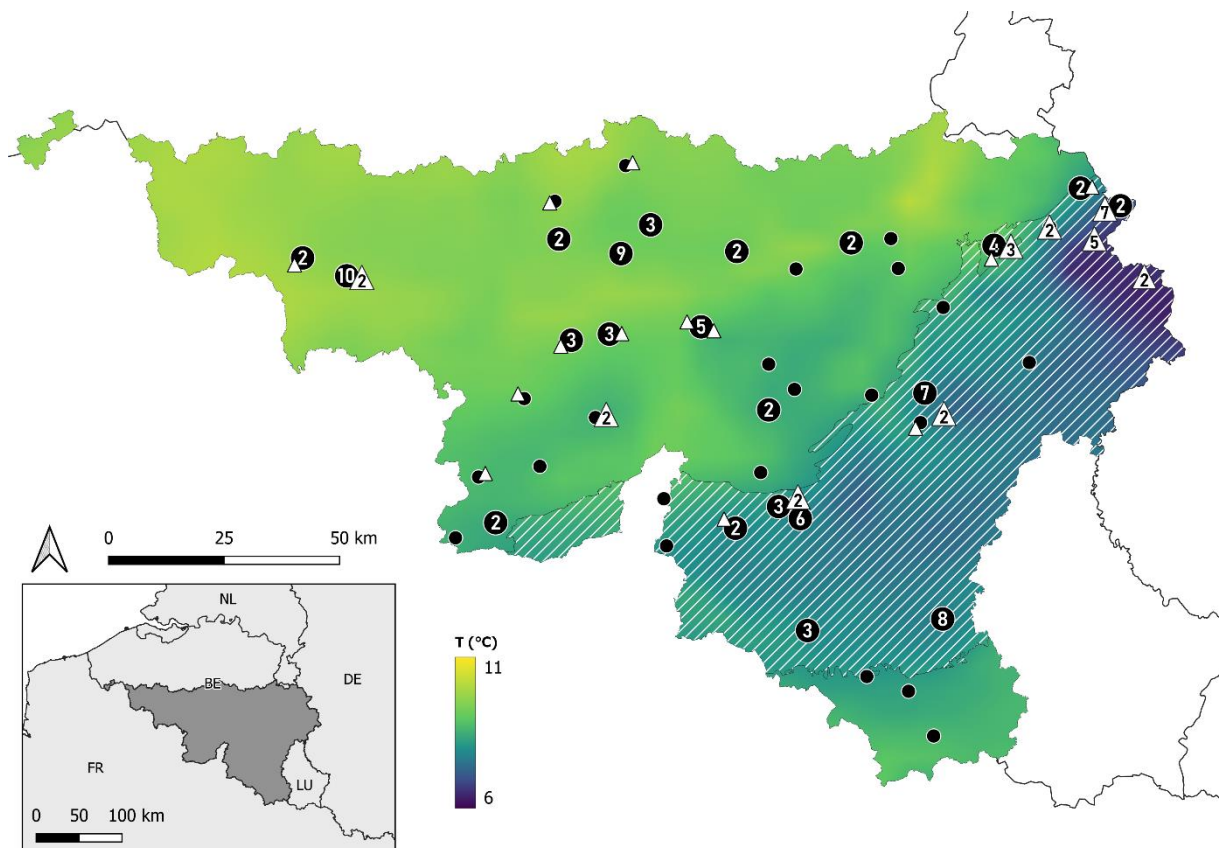
108 available, the geocentric approach is a cost-effective way to predict site index over large areas
109 (e.g. Aertsen et al., 2012; Parresol et al., 2017).

110 Although birch productivity is well documented in the northern regions (Eriksson et al., 1997;
111 Karlsson et al., 1997; Lee et al., 2024; Liziniewicz et al., 2022), this important information
112 remains poorly explored in other parts of its distribution range (Diéguez-Aranda et al., 2006;
113 Hein et al., 2009), particularly in northwestern Europe where birch silviculture is gaining
114 popularity. Our study has two main objectives: (i) develop a model for predicting *B.pendula*
115 site index based on dominant height and age using a phytocentric approach; (ii) develop a
116 second model identifying the key biophysical factors affecting *B.pendula* site index through a
117 geocentric approach. This model was ultimately used to map the spatial variation in birch yield
118 potential in the study area.

119 2 Material and Methods

120 2.1 Study area

121 The study area was located in southern Belgium of northwestern Europe (Fig. 1). The sites
122 covered a wide range of ecological conditions and were distributed across two ecoregions,
123 known as the lowlands and the uplands (Campioli *et al.*, 2012). The lowlands ecoregion was
124 characterized by low elevations (173 ± 88 m), the lowest amount of rainfall (863 ± 84 mm) and
125 the highest temperature (9.2 ± 0.5 °C) while the uplands ecoregion was characterized by high
126 elevations (428 ± 90 m), low temperatures (7.7 ± 0.5 °C) and high amounts of rainfall (1105 ± 110
127 mm). The study focused on silver birch (*Betula pendula* Roth.), but due to similar
128 morphological characteristics, some individuals may belong to downy birch (*Betula pubescens*
129 Ehrh.), the other birch species found in Belgium.



130
131 *Fig. 1: Birch locations in southern Belgium for the phytocentric (triangular white dots) and*
132 *geocentric approach (round black dots) with mean annual temperature over the 30-year period*

133 1961-1990. Numbers indicate several dots close to each other. Striped area indicates the
134 uplands ecoregion within the study area.

135 2.2 Phytocentric approach

136 The phytocentric approach consisted in collecting records of height and age of dominant trees
137 with stem analysis (section 2.2.1) and modelling the relationship between height (H_{DOM}) and
138 age (Age; Eq. 1; section 2.2.2) of dominant trees. Each model included the b_i parameter that
139 was fitted individually for each stand i and that expressed stand productivity level (Perin *et al.*,
140 2013).

$$141 H_{\text{DOM}} = f(\text{Age}, b_i, a, c, d, p, r) \quad (1)$$

142 with a, c, d, p, r the fixed parameters.

143 For any pair of Age and H_{DOM} , b_i could be estimated by inversion of eq. 1 (Eq. 2):

$$144 b_i = f(H_{\text{DOM}}, \text{Age}, a, c, d, p, r) \quad (2)$$

145 With H_{DOM} and Age corresponding to the dominant height and age of an even-aged stand i .

146 Consequently, combining eq. 1 and eq. 2, the dominant height reached at the reference age, i.e.
147 the site index could be estimated (Eq. 3):

$$148 SI_i = H_{\text{DOM}} \text{ at } \text{Age}_{\text{ref}} = f(H_{\text{DOM}}, \text{Age}, \text{Age}_{\text{ref}}, a, c, d, p, r) \quad (3)$$

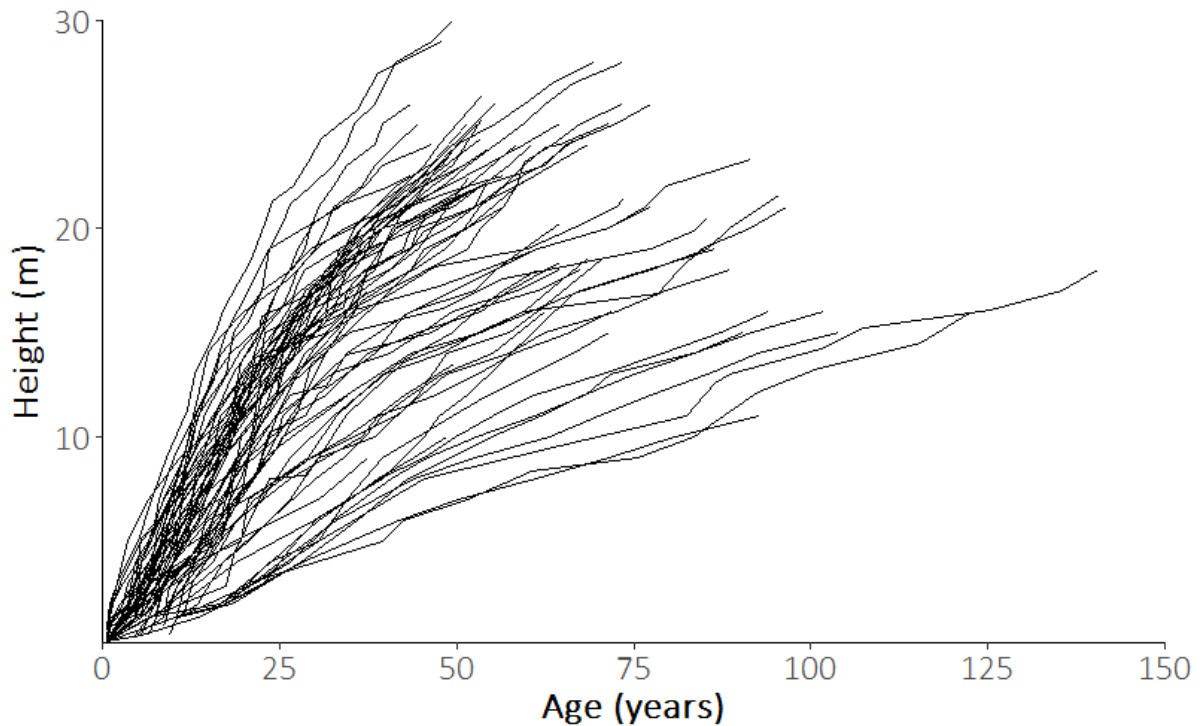
149 With SI_i corresponding to the site index and Age_{ref} to the chosen reference age.

150 2.2.1 Stem analysis

151 Stem analyses (SA) were used to reconstruct the past height growth of birch trees (Fig. 2). The
152 trees for SA were selected from 40 even-aged stands covering most of the birch range and
153 geographical locations, with elevation ranging from 63.9 m to 601.6 m and from acid peaty
154 soils to well-drained rich soils (triangular white dots in Fig. 1). 23 stands were sampled in 2004
155 and 17 more stands in 2019 and 2020. For each stand, sampling points were established within
156 small homogeneous groups of birch trees covering 0.1 ha. SA were conducted within plots of
157 500 m² centered on these homogeneous groups to minimize edge effects from surrounding

158 stands. For logistical reasons, the number of trees sampled per plot was limited to three, with
159 an average of two trees per plot. This corresponds to the 60 largest trees per hectare, with an
160 average of 40 largest trees per hectare. Although this approach differs from the usual definition
161 of stand dominant height - the mean height of the 100 largest trees per hectare - it has already
162 been suggested as appropriate for small-sized sampling units or cases where only a few leading
163 trees can be measured (Carmean, 1996; Le Goff *et al.*, 1982). For every cut tree, stem disks
164 were collected at the base (0.2 or 0.5 m) as well as at breast height (1.3 m). Subsequent disks
165 were collected with 2 m intervals up to the top of the tree. The name of the sample plot, the tree
166 number and disk height were written on the non-working surface of the disks. The disk
167 thickness was approximately 8 cm (4 cm above and 4 cm below the line). The disks were placed
168 in a cool and ventilated place for drying to prevent fungi development.

169 After being air-dried, the working surfaces of the disks were planed and progressively sanded
170 (grit 80-320). For the disks collected in 2004, the number of rings was counted on 2 to 3 paths
171 from pith to bark on each disk using a binocular microscope. The disks from later samplings
172 (2019 and 2020) were scanned at high resolution (≥ 1200 DPI) with an Epson® scanner
173 (10000XL), rings were then counted on different paths using the WinDendro® 2021 software
174 (Regents Instruments). Birch trees that had uncertain age estimates due to heart rot, or had
175 anomalies in the growth trajectories were excluded from the dataset. As cross-section lengths
176 did not coincide with periodic height growth, the height-age data from the SA were corrected
177 following the method proposed by Salas-Eljatib (2021). The resulting dataset characteristics
178 can be found in Table 1.



179

180 *Fig. 2: Observed height-age series from the stem analysis of the 68 birch trees sampled in 40*
 181 *stands in southern Belgium.*

182 *Table 1: Summary statistics of stands used in stem analyses for lowlands and uplands.*

	Lowlands	Uplands
No. of sites	14	26
No. of trees	29	39
No. of paired age-height records	526	495
Mean age \pm sd (years)	58.7 \pm 10.4	69.7 \pm 25
Mean height \pm sd (m)	24.7 \pm 2.5	19.1 \pm 3.8
Mean altitude \pm sd (m)	188.6 \pm 82.9	459.8 \pm 112.3

183

184 2.2.2 Dominant height growth curves

185 We tested 16 commonly used non-linear models to predict dominant height growth in response
 186 to tree age (Table 2; Perin et al., 2013). All functions were fitted using non-linear mixed effects
 187 models computed with the *nlme* R package (Pinheiro et al., 2024). We addressed the first order
 188 autocorrelation (i.e., the height reached at age n is correlated with the height reached at age n -

189 I) and heteroscedasticity using a continuous autoregressive correlation structure as well as a
190 variance power function of total age. A parameter b was estimated for each stand (i.e., $b \sim \text{stand}$
191 in the fixed parameters of the nlme function) and a tree-level random effect was added to this
192 parameter to account for differences between SAs performed in the same stand (i.e., $b \sim 1 | \text{tree}$ in
193 the random parameters of the nlme function). The other parameters (a, c, d, p, r), hereafter
194 referred to as model fixed parameters, were considered as fixed effects and, for each of them, a
195 unique value was fitted over the whole dataset.

196 The statistical performance of the tested models was assessed examining the maximized log-
197 likelihood (LogLik), the Akaike Information Criterion (AIC), the root-mean-square error
198 (RMSE) and the distribution of residuals.

199 The best model was selected based on the overall consideration of the aforementioned criteria.

200 We verified that the model fixed parameters had value significantly different from zero (p -
201 value < 0.05 ; Table A1). Furthermore, we assessed the trend in the residuals of the best selected
202 model as a function of age and ecoregion (lowlands and uplands; see Fig. 1) using an analysis
203 of covariance. This test was performed to determine whether the model fitting should also
204 depend on the ecoregion.

205 *Table 2: Names, abbreviations and mathematical formulations of all model functions tested on*
 206 *the SA dataset. The productivity level parameter corresponds to b_i whereas a , c , d , p and r are*
 207 *model fixed parameters.*

Name	Abbreviation	Mathematical equation
Mitscherlich	M	$b_i * \left(1 - \exp\left(\frac{(a - Age)}{c}\right)\right)$
Gompertz	G	$b_i * \exp\left(-\exp\left(\frac{(a - Age)}{c}\right)\right)$
Modified Gaussian	MG	$b_i * \left(1 - \exp\left(-\left(\left(\frac{(Age - a)}{c}\right)^2\right)\right)\right)$
Log-logistic	Log	$\frac{b_i}{\left(1 + \left(\frac{Age}{a}\right)^{-c}\right)}$
Arc-tangent	Arc	$\left(\frac{b_i}{\pi}\right) * \left(\frac{\pi}{2} + \text{atan}\left(\frac{(Age - a)}{c}\right)\right)$
Hyberpolic amplitude	Hyp	$\left(\frac{b_i}{\pi}\right) * \left(\frac{\pi}{2} + \text{asin}\left(\tanh\left(\frac{(Age - a)}{c}\right)\right)\right)$
Johnson Schumacher	JS	$b_i * \exp\left(\frac{-c}{(Age - a)}\right)$
Chapman-Richards anamorphic	CN	$b_i * (1 - \exp(-a * Age))^c$
Chapman-Richards polymorphic	CP	$a * (1 - \exp(-b_i * Age))^c$
Bailey and Clutter anamorphic	BN	$\exp\left(b_i + a * \left(\frac{1}{Age}\right)^c\right)$
Bailey and Clutter polymorphic	BP	$\exp\left(a + b_i * \left(\frac{1}{Age}\right)^c\right)$
Duplat and Tran-Ha I	DTI	$(a * Age + b_i) * \left(1 - \exp\left(-\left(\frac{Age}{c}\right)^d\right)\right)$
Duplat and Tran-Ha II	DTII	$(a * Age + b_i) * \left(1 - \exp\left(-\left(\frac{Age}{c}\right)^d\right)\right) + p * Age$
Duplat and Tran-Ha III	DTIII	$(a * Age + b_i) * \left(1 - \exp\left(-\left(\frac{Age}{c}\right)^d\right)\right)^r + p * Age$

Duplat and Tran-Ha IV	DTIV	$(a * \ln(Age) + b_i) * \left(1 - \exp\left(-\left(\frac{Age}{c}\right)^d\right)\right)$
Duplat and Tran-Ha V	DTV	$(a * \ln(Age) + b_i) * \left(1 - \exp\left(-\left(\frac{Age}{c}\right)^d\right)\right) + p * Age$

208

209 2.2.3 Selection of a reference age

210 The reference age used to compute SI is commonly set at 50 or 100 years for long-lived tree
 211 species such as spruce, oak and beech (Albert and Schmidt, 2010; Seynave et al., 2008).
 212 However, this age cannot be used to define the site index for birch, whose longevity rarely
 213 exceeds 100 years and for which recommended rotation are between 50 and 60 years (Dubois
 214 et al., 2021). We chose a reference age of 30 years following the recommendations of (Goelz
 215 and Burk, 1992) (see Appendix B). This reference age also corresponded to the end of the
 216 maximum growth phase of birch (Wilhelm and Rieger, 2023).

217 2.2.4 Cross-validation

218 The validation of the best model was performed using a repeated k-folds cross validation
 219 procedure which is assumed to be more accurate and reliable for the estimation of predictive
 220 accuracy compared to the simple k-folds cross validation (Nakatsu, 2021). The dataset was
 221 randomly divided into k=4 roughly equal-sized parts (17 trees), three folds being used for model
 222 training (training dataset) which is then applied to the remaining part (validation dataset). The
 223 best model formula (section 2.1.1) was fitted on each training dataset, resulting in four models
 224 and four set of fixed parameters (a,c,d,p,r) . For each tree in the validation dataset, the b
 225 parameter was estimated based on the fixed parameters by inverting the mathematical equation
 226 (Eq. 2). The b parameter was estimated using the age-height couple for which the age was the
 227 closest to the best reference age found in section 2.1.3. Once b parameter was estimated, it was
 228 possible to predict the dominant height (Eq. 1) for all other age-height couples for each tree of

229 the validation dataset. For each validation dataset, the mean error (mean of the residuals; ME)
 230 and RMSE were calculated based on the observed and predicted heights.
 231 The whole procedure was repeated 10 times, resulting in 40 validation ME and RMSE which
 232 were averaged and used as indicators of the model predictive performance.

233 2.3 Geocentric approach

234 Using additional plot data and the fitted dominant height growth curves (section 2.2.2), the SI
 235 (Eq. 3), a proxy of birch productivity, was estimated for 103 stands and modeled in response to
 236 variables describing biophysical conditions (Eq. 4).

$$237 \text{SI} = f(\text{edaphic, climatic, topographic}) \quad (4)$$

238 2.3.1 Sampling design

239 This approach was applied to 103 circular plots (Table 3), in even-aged stands located across
 240 southern Belgium (round dots in Fig. 1). For each stand, dominant height was calculated based
 241 on the 100 largest trees per ha whereas stand age was obtained by counting rings on increment
 242 cores collected from one or two dominant trees.

243 *Table 3: summary statistics of the 103 sample plots for the geocentric approach*

	Mean	Standard deviation	Minimum	Maximum
Age (years)	45	14	21	94
Dominant height (m)	21.2	3.9	9.3	28.9
Circumference at 1.3m (cm)	84	29	35	177
Site index (m)	16.9	2.9	7.0	24.6
Plot area (m ²)	557	354	30	2324
Number of trees per ha	737	637	96	2333

244

245 2.3.2 Variables extraction

246 Using the equation developed in section 2.2.2, the b parameter was estimated for each stand
 247 based on its age and dominant height, and the site index (dominant height at 30 years; response
 248 variable) was then calculated.

249 Meteorological data were extracted from databases of the Royal Meteorological Institute of
250 Belgium. We computed several climatic variables over the 30-year period from 1961-1990,
251 which was assumed as the period having mostly influenced trees growth until they reached the
252 reference age of 30 years (see section 2.2.3). Based on daily observational gridded data with a
253 spatial resolution of 5 km (Journée et al., 2019), the following variables were determined for
254 each stand location: mean annual temperature (MAT; °C), mean April-September (growing
255 season) temperature (GST; °C), annual precipitation (PREC; mm) and April-September
256 precipitation sum (GSP; mm), summer water balance (SWB; mm) and growing season length
257 (GSL; days). The SWB corresponded to the difference between the precipitation and the
258 potential evapotranspiration during the period April-September. The GSL was calculated
259 according to European Climate Assessment (Schulzweida and Quast, 2015), as the difference
260 between the first day with a mean temperature exceeding 10°C for at least 6 consecutive days
261 and the first day with mean temperature below 10°C for at least 6 consecutive days (within the
262 last 6 months).

263 A topographic categorical variable was included in the analysis. This variable was obtained
264 from a 10 m resolution digital map classifying the landscape into four categories: cold north-
265 east facing slopes (NESLP), south-west facing slopes (SWSLP), neutral sites (NS) and valley
266 bottom (VB; Wampach et al., 2017).

267 Edaphic variables potentially influencing tree growth were also included in the analysis. Forest
268 soil nutrient availability (NUT), obtained from spatial data with a resolution of 10 m, was
269 classified into four categories: hyper-oligotrophic soils (H-OLIGO), oligotrophic soils
270 (OLIGO), lightly acidic soils (ACID), and mesotrophic to rich soils (MESO; Lisein et al.,
271 2022). We also considered the soil depth (SD; cm) and the maximal soil water content (SWC;
272 mm), which were available as spatial data with a resolution of 10 m (Legrain et al., 2014;

273 Ridremont et *al.*, 2011). SWC depended on the soil texture, stoniness and the maximum depth
274 of the soil profile. Summary statistics of all variables are presented in Table 4.

275 *Table 4: Summary statistics of biophysical variables used in the geocentric approach*

Type	Class	Variable	Description	Mean	St.dev.	Min	Max
Continuous	Climatic	MAT	Mean annual temperature (°C)	8.64	0.70	7.07	9.66
		GST	April-September mean temperature (°C)	13.24	0.61	11.78	14.17
		PREC	Precipitation sum (mm)	950.0	140.9	774.7	1268.0
		GSP	April-September precipitation sum (mm)	453.2	50.9	387.7	597.0
		GSL	Growing season length (days)	184.5	9.3	163.6	200.7
		SWB	Summer water balance (mm)	-17.25	54.07	-92.18	143.0
	Edaphic	SD	Soil depth (cm)	87.82	35.21	20.00	125.00
		SWC	Soil water content (mm)	152	76	14	261
Type	Class	Variable	Description	Levels	No. observation		
Categorical	Topographic	TOPO	Topographic position	NESLP	4		
				SWSLP	9		
				NS	81		
				VB	9		
	Edaphic	NUT	Nutrient availability	H-OLIGO	12		
				OLIGO	38		
				ACID	31		
				MESO	22		

277 2.3.3 Statistical analyses

278 The climatic, topographic and edaphic variables were used to develop a geocentric model in
279 order to predict SI using generalized additive models (GAM) with the *mgcv* package in R
280 (Wood *et al.*, 2016). This statistical tool provides flexibility in cases of non-linear relationships
281 between predictors and the response variable. As a first step, different models were built with
282 all variables, except those with Pearson's correlations values exceeding 0.7 or -0.7, in order to
283 avoid collinearity (Figure S2). Then, a manual backward stepwise approach was used to remove
284 variables according to the AIC value. The best model was selected based on the lowest AIC
285 value and the smallest number of retained variables, ensuring a parsimonious and easily
286 interpretable model. An interaction term was investigated between the remaining climatic and
287 soil variables. We verified model assumptions examining model residuals over predicted
288 values. Using 10 repeated 5-fold cross-validations, we calculated the RMSE and adjusted R²
289 for each model to estimate its prediction error and the percentage of variance explained by the
290 selected predictors (Table S4).

291 2.3.4 Mapping predictions of the site index in southern Belgium

292 The best geocentric model was used to produce maps of the potential SI of silver birch over the
293 study area for the reference period 1961-1990 and by considering an increase of 1.5°C in mean
294 annual temperature compared to this reference period. To do so, a regular grid of points spaced
295 100 m apart was generated across southern Belgium. For each point, the values of model
296 variables were extracted, and SI (the dominant height at 30 years) was then predicted using our
297 geocentric model. The SI predictions were categorized based on whether they fell within the
298 model's calibration domain. Predictions within the calibration domain corresponded to mean
299 annual temperature (MAT) and soil water content (SWC) values within the range of the
300 observations. Predictions outside the calibration domain were further subdivided: those within
301 the observed range of SI values and those outside the observed range of SI. Predictions in this

302 latter category were excluded and highlighted using a unique color for clarity. All predictions
303 were rasterized using the R package *Stars* (Pebesma and Bivand, 2023). For illustrative
304 purposes, the same methodology was applied to produce a second predictive map assuming a
305 1.5°C increase in MAT, the other model variable (SWC) remaining unchanged. The two
306 predictive maps were then used to calculate and illustrate the percentage increase in SI
307 associated with the 1.5°C temperature rise. Additionally, for each predictive map, the associated
308 GAM standard error map was also produced.

309 **3 Results**

310 **3.1 Phytocentric approach**

311 **3.1.1 Dominant height growth models**

312 The models based on the Duplat and Tran-Ha equations (DTI, DTII, DTIII, DTIV, DTV:
313 described in Table 2) presented the best statistics, with the lowest AIC, LogLik and RMSE
314 values (Table 5). Although the model based on the modified Gaussian equation ranked first
315 according to the AIC criteria, the RMSE was among the worst. Models based on Arc-tangent
316 and hyperbolic equations (Arc, Hyp) performed relatively poorly as indicated by their high AIC
317 and RMSE values and their low LogLik values (Table 5). The other models (G, CP, CN, M,
318 Log, JS, BN, BP) showed similar but lower performance statistics.

319 The models based on the DTI, DTII and DTV equations presented very similar performance.
320 The DTV model ranked second according to the AIC and logLik criteria, followed by the DTI
321 and DTII models. The DTI model had fewer fixed parameters (a, c, d) compared to the DTII
322 and DTV models (a, c, d, p), which helps to avoid over-parameterization. After a visual
323 inspection of the residuals, the DTI model was selected for predicting dominant height. The
324 analysis of covariance showed no significant difference between the residuals for the stands
325 located in the lowlands and in the uplands (Table A2). Dominant height growth curves,
326 developed for site index values of 5, 10, 15 and 20 m at 30 years, were well representative of
327 birch potential productivity in Belgium (Fig. 3).

328 The residuals of the DTI growth model showed no heteroscedasticity in the range of height
329 prediction (Figure A1). Across all age classes, the mean value of residuals remained below 0.5
330 m, indicating the DTI model's strong performance across various age ranges (Figure A2). The
331 fixed parameters (a, c, d) in the best model were highly significantly different from zero, leading
332 us to retain all of them (Table A1).

333 The formulation of the best model (DTI) was:

334
$$H_{DOM} = (a * Age + b_i) * \left(1 - \exp\left(-\left(\frac{Age}{c}\right)^d\right)\right) \quad (5)$$

335 where H_{DOM} was the dominant height (in m); Age was the stand age; a , c , d were the model
 336 fixed parameters; b_i was the site-specific parameter depicting stand productivity.

337 The productivity level of a given stand can be calculated for any dominant height-age pair, with
 338 an inversion of Eq. 5:

339
$$b_i = \frac{H_{DOM}}{1 - \exp\left(-\left(\frac{Age}{c}\right)^d\right)} - a * Age \quad (6)$$

340 The SI of a given stand was found by combining Eq. 5 and Eq. 6:

341
$$SI = \left(a * (Age_{ref} - Age) + \frac{H_{DOM}}{1 - \exp\left(-\left(\frac{Age}{c}\right)^d\right)} \right) * \left(1 - \exp\left(-\left(\frac{Age_{ref}}{c}\right)^d\right)\right) \quad (7)$$

342 where Age_{ref} is the selected reference age (chosen to be 30 years).

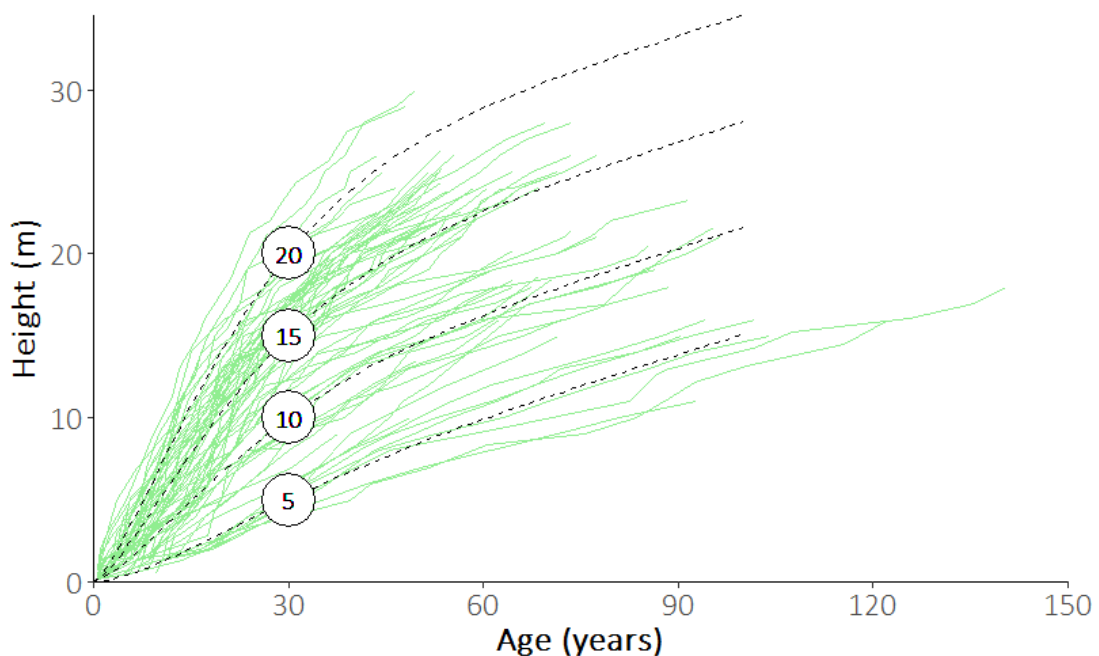
343 The results of the cross-validation for the DTI model indicated a RMSE of 1.41 m and a ME of
 344 -0.024 m (Table S1).

345

346 *Table 5: Akaike Information Criterion (AIC), maximised log-likelihoods (LogLik) and root*
 347 *mean square error (RMSE; m) for all models tested on the SA dataset.*

Model	AIC	LogLik	RMSE	Δ AIC
MG	2506.4	-1207.2	4.03	0.0
DTV	2506.9	-1205.4	1.22	0.5
DTI	2507.3	-1206.6	1.23	0.9
DTII	2508.0	-1206.0	1.22	1.6
DTIII	2513.5	-1207.8	1.33	7.1
DTIV	2533.2	-1219.6	1.26	26.8
BP	2552.8	-1230.4	1.39	46.4
CP	2557.2	-1232.6	1.38	50.7
BN	2581.7	-1244.8	1.47	75.3
JS	2588.6	-1248.3	1.47	82.2
Log	2590.2	-1249.1	1.48	83.7
M	2604.7	-1256.4	1.55	98.3
CN	2607.4	-1257.7	1.50	100.9
G	2720.2	-1314.1	1.74	213.8
Hyp	2839.7	-1373.9	2.32	333.3
Arc	2898.4	-1403.2	3.04	392.0

348



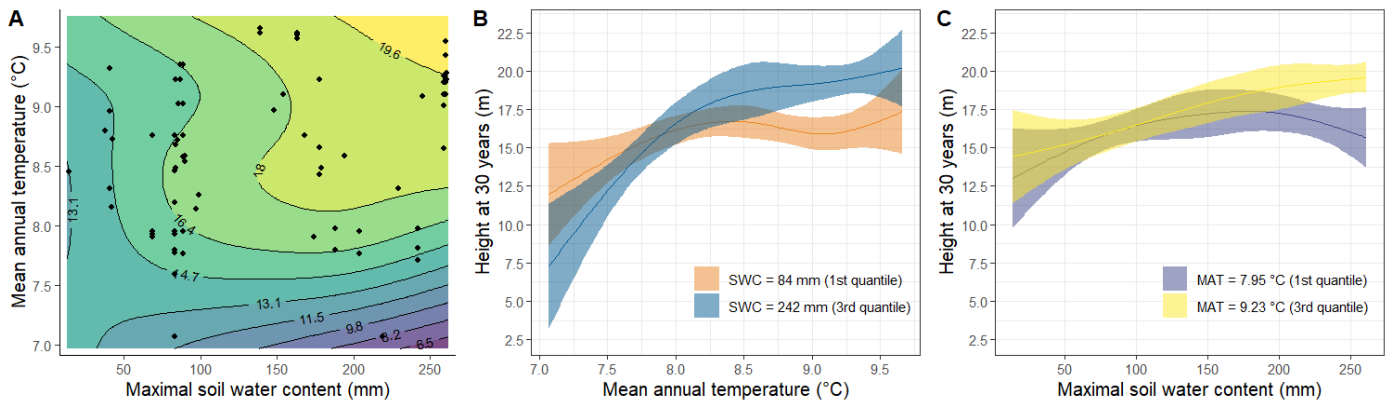
349

350 *Fig. 3: Duplat and Tran-Ha I model height trajectories corresponding to given values of site*
 351 *index (5, 10, 15 and 20 m at a reference age of 30 years, dashed lines). These model predictions*
 352 *were superposed on the observed height growth series from stem analysis (green solid lines).*

353 3.2 Geocentric approach

354 3.2.1 Effects of climate and soil factors on birch productivity

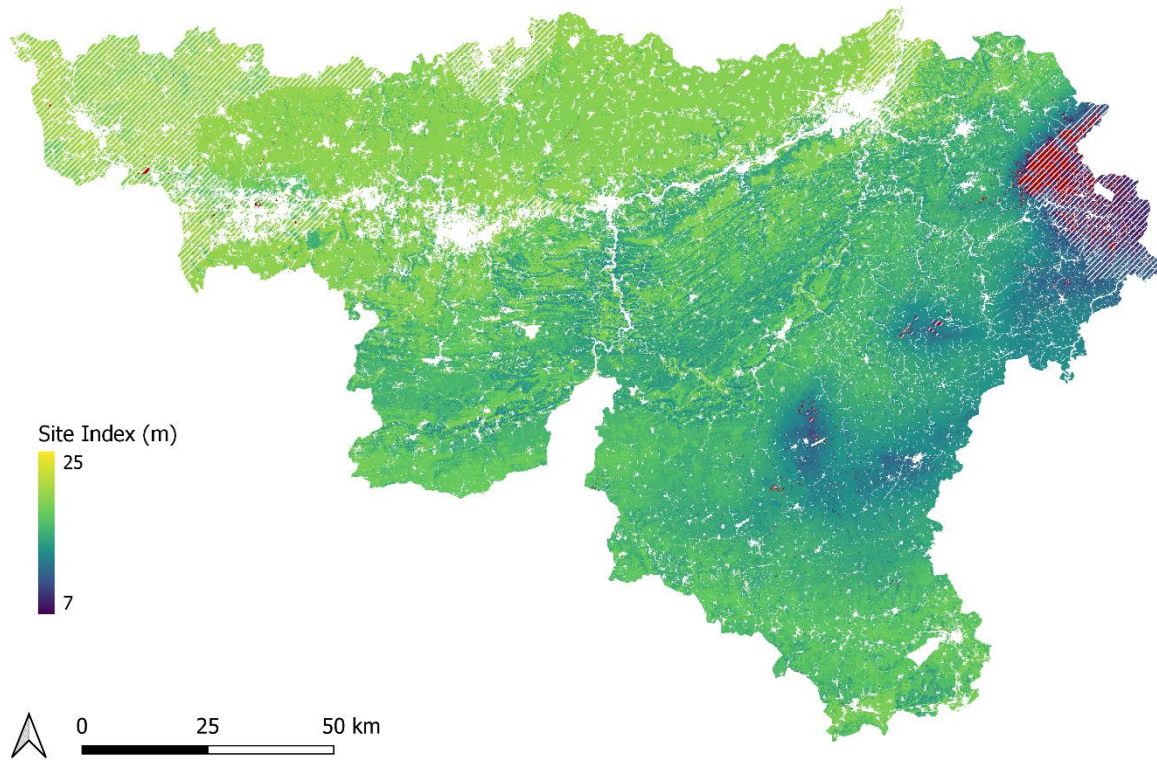
355 The stepwise selection procedure identified the best model as the one including a climatic
356 variable, the mean annual temperature (MAT) interacting with an edaphic variable, the maximal
357 soil water content (SWC) (Table S3). This model explained 55 percent of the deviance (Table
358 C1) and the examination of residuals over predicted values did not reveal any particular trend
359 (Figure C1). The positive effect of temperature on the SI depended on the value of the maximal
360 soil water content considered. The positive effect of temperature on the SI was limited for SWC
361 values below 100 mm (Fig. 4A). For a given and low value of SWC (84 mm), the increase in
362 mean annual temperature led to a small increase in SI, while this increase was stronger for a
363 high value of SWC (242 mm). Above 8°C in MAT, the increase in SI became less pronounced
364 for a given and high value of SWC (242 mm), while the SI tended to decrease slightly from this
365 threshold temperature when a low value of SWC (84 mm) was considered. Specifically, below
366 8°C, the increase in SI was about 10 m per degree for a SWC value of 242 mm, whereas the
367 increase was much lower for a SWC value of 84 mm, at about 5 m per degree (Fig. 4B). The
368 increase in SWC had a positive effect on the site index, particularly pronounced from 8°C in
369 MAT (Fig. 4A). For a given mean annual temperature value of 7.95°C, the SI started to decrease
370 from a SWC value of about 200 mm (Fig. 4C).



371 *Fig. 4: Biophysical factors driving birch site index (dominant height at 30 years; predicted*
 372 *values in m) in southern Belgium. (A) Contour plot showing the effect of interaction between*
 373 *the mean annual temperature (MAT; °C) and the maximal soil water content (SWC; mm) on*
 374 *site index values; black dots correspond to the observations. (B) Effect of MAT on site index*
 375 *for two levels of SWC: the first quantile (84 mm) and the third quantile (242 mm). (C) Effect of*
 376 *SWC on site index for two levels of MAT: the first quantile (7.95°C) and the third quantile*
 377 *(9.23°C).*

378 3.2.2 Mapping predictions of the site index in southern Belgium

379 The highest productivity (≈ 20 m at 30 years) was found in the northern and southernmost parts
380 of the study area. Intermediate values of site index (≈ 15 m at 30 years) were encountered in
381 the uplands (hatched area in Fig. 1) while the lowest values (≈ 10 m at 30 years) were mainly
382 found in the eastern part (Fig. 5). The standard error was less than 1.63 m for 90 percent of the
383 predictions within the study area for the reference period (1961-1990) and less than 7.21 m with
384 1.5 additional degrees in MAT (Figure S6; Figure S7). Regarding the reference period, part of
385 the east and some areas in the west were outside the model's calibration range, representing a
386 total of 13 % of the study area. The majority of predictions outside the range of observed SI
387 values were in the east, accounting for about 1% of the study area (Fig. 5). These values
388 increased to 71% and 0.2% respectively for the 1.5 additional degrees scenario. The part of the
389 study area that remained within the model calibration range roughly corresponded to the upland
390 ecoregion (Figure S5).



391

392 *Fig. 5: Predicted site index (dominant height at 30 years in m) for silver birch in southern*

393 *Belgium. White striped areas are those outside the model's calibration domain (MAT or SWC*

394 *value lower [higher] than the minimum [maximum] value used to calibrate the model).*

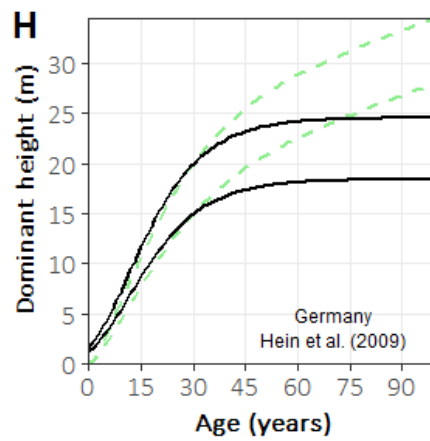
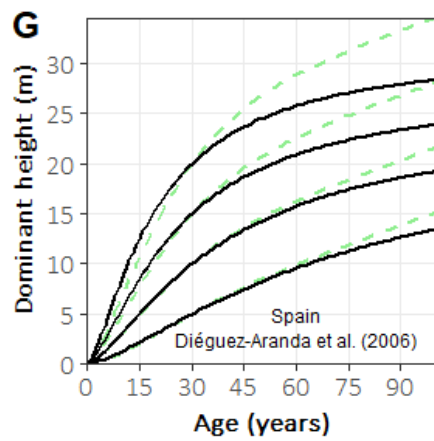
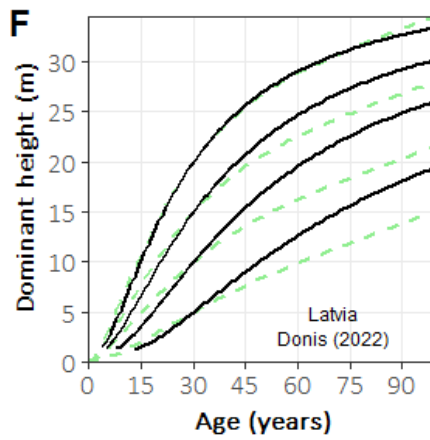
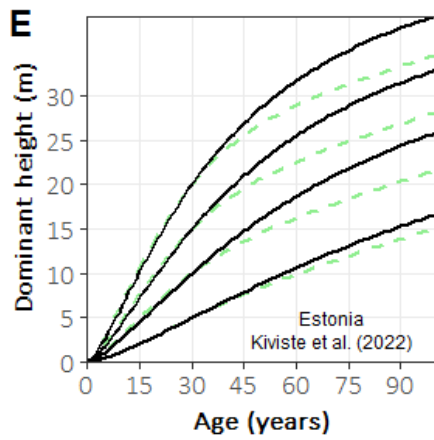
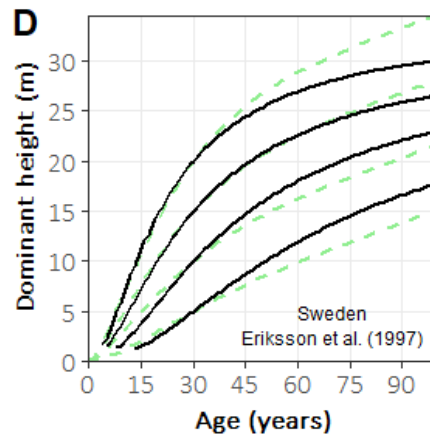
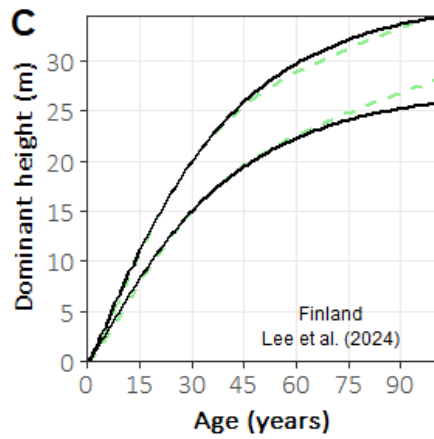
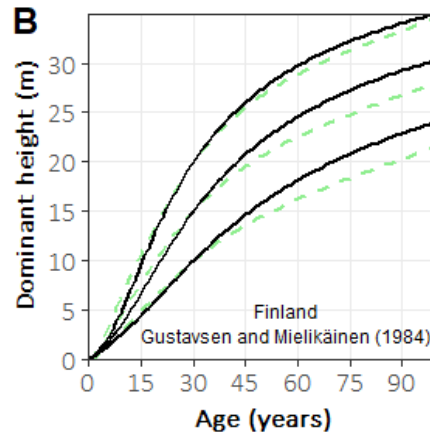
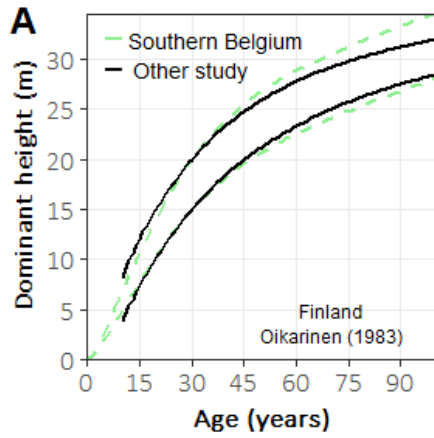
395 *Predictions outside the range of observed values of site index are displayed in red.*

396 4 Discussion

397 4.1 Phytocentric approach

398 The Duplat and Tran-Ha equations appeared best suited to model dominant height trajectories
399 (Table 5). In accordance with previous studies examining the dominant height growth of other
400 broadleaved species such as cherry and sycamore maple (Claessens *et al.*, 1999) and softwood
401 species such as spruce and larch (Perin *et al.*, 2013; Zhang *et al.*, 2022), the complexity of these
402 models - having more parameters than the other tested models - seems required to fit the data.
403 The estimated site index curves of our study were compared to those of other previous studies
404 by fixing the SI at a reference age of 30 years (Fig. 6). The different site index curves show
405 similar growth patterns with an early rapid height growth followed by a gradual decrease, which
406 is typical for pioneer tree species. However, differences in growth patterns are observed and
407 may be explained by local variations in the height growth dynamics, the type of data used to
408 develop productivity curves (permanent sample plots, temporary sample plots, or stem
409 analysis), the type of model (sigmoidal or non-sigmoidal), and the birch species studied (silver
410 birch, downy birch, or a combination of both). Among the studies reviewed, only the
411 productivity curves from Eriksson *et al.* (1997), Diéguez-Aranda *et al.* (2006), and Hein *et al.*
412 (2009) were constructed using stem analysis, while the others relied on permanent or temporary
413 sample plots. Among the studies based on stem analysis, the growth pattern described by the
414 German model differs most significantly from ours, notably due to its horizontal asymptote,
415 which is absent in the other productivity curves. Furthermore, similar to the situation in
416 Wallonia, the productivity curves of Gustavsen and Mielikäinen (1984), Donis (2022), Eriksson
417 *et al.* (1997), and Kiviste *et al.* (2022) were developed for both birch species combined, whereas
418 those of Lee *et al.* (2024), Oikarinen (1983), and Hein *et al.* (2009) were specifically calibrated
419 for silver birch, and Diéguez-Aranda *et al.* (2006) curves were fitted exclusively for downy
420 birch. Additionally, the models of Oikarinen (1983) and Gustavsen and Mielikäinen (1984) are

421 not based on sigmoidal growth functions, unlike those used in the other studies. Finally, it is
422 important to highlight that these differences may also be due to the sampling, notably the age
423 range. It should be noted that, in the most fertile conditions, our model shows more sustained
424 growth than most of the other models. Indeed, we sampled mostly relatively young trees (<50
425 years) for the higher productivity classes. Beyond 50 years, the height growth is extrapolated
426 which makes the comparison with other models at these ages less accurate. This reflects a
427 common sampling bias where higher productivity classes are generally represented by younger
428 trees, while lower productivity classes tend to include older trees (Socha et al., 2016).



430 *Fig. 6: Comparison of the dominant height growth curves of this study for site index values at*
431 *a reference age of 30 years and other published dominant height growth curves from Sweden*
432 *(Eriksson et al., 1997*), Finland (Gustavsen and Mielikäinen, 1984; Lee et al., 2024;*
433 *Oikarinen, 1983), Estonia (Kiviste et al., 2022), Latvia (Donis, 2022*), North-Western Spain*
434 *(Diéguez-Aranda et al., 2006) and Germany (Hein et al., 2009).* Site index curves were*
435 *developed from breast height age instead of stump age as is our case. To compare their curves*
436 *with our own, we thus applied correction ages, being the time needed for a birch to grow from*
437 *stump to breast height, of 12, 7, 4 and 3 years for 5, 10, 15 and 20 m site indices classes*
438 *respectively.*

439 4.2 Geocentric approach

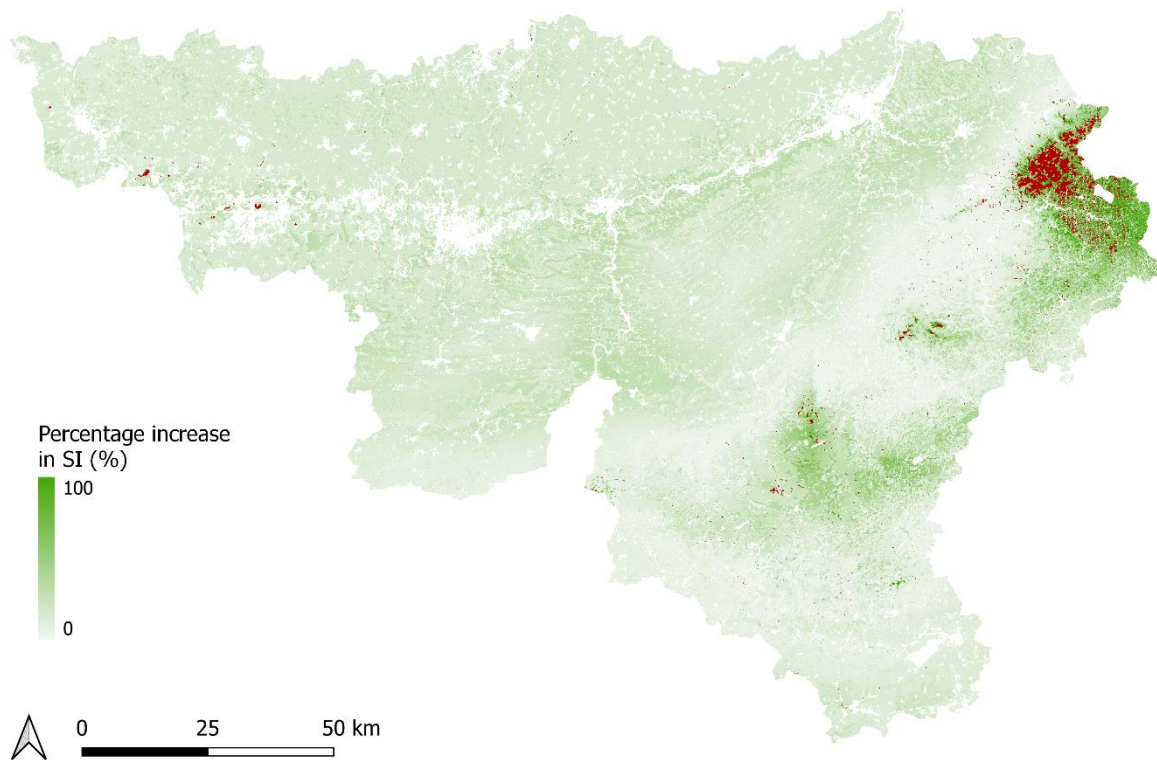
440 The geocentric approach highlighted the key biophysical factors influencing birch growth: a
441 climatic variable, the mean annual temperature interacting with an edaphic variable, the
442 maximal soil water content.

443 In northwestern Europe, birch productivity seems to be promoted by the increase in mean
444 annual temperature (Fig. 4B). This result is in line with previous studies, which have also
445 reported a positive effect of temperature on height growth, as a warmer climate can especially
446 lead to a longer growing season (Albert and Schmidt, 2010; Álvarez-Álvarez et al., 2011;
447 Brandl et al., 2018; Combaud et al., 2024; Pau et al., 2022). The stimulating effect of
448 temperature on growth tends to saturate after 8°C (Fig. 4B) for silver birch. This saturation
449 effect could be attributed to temperature ceasing to be a limiting factor for growth, or because
450 rising temperatures may increase evapotranspiration, hydric stress, and reduce photosynthetic
451 activity (Lindner et al., 2010). In this study, we were not able to capture a reverse effect of
452 further warming on birch growth given that our climatic range might be insufficient, underlining

453 the importance of extending the study area, particularly in the southern part of the distribution
454 range (Fontes et al., 2010).

455 The positive effect of temperature on birch productivity is likely limited by soil water
456 availability. The interaction between temperature and soil water content moderated the positive
457 effect of temperature (Fig. 4A), suggesting that birch growth could be constrained by low soil
458 water availability in warmer regions of northwestern Europe, as trees tend to limit
459 evapotranspiration to avoid water loss and the risk of cavitation (Brandl et al., 2018). In the
460 lowland ecoregion of southern Belgium, warmer temperatures lead to a longer growing season,
461 promoting height growth. Soil is generally loamy and deep with sufficient water content,
462 protecting the trees from water shortage in drought periods. However, a warmer climate will
463 not necessarily increase productivity in this ecoregion, as temperature is not the main growth-
464 limiting factor (Fig. 7). Birch silviculture may thrive on sites where soil water content does not
465 limit growth.

466 In the northern part of its distribution range, where growth is limited by low temperatures, silver
467 birch may eventually benefit from rising temperatures, especially in stands characterized by
468 high soil water content (Fig. 4C; Fig. 7). Currently, the uplands ecoregion shows low
469 productivity values (10 m-15 m at 30 years) because of low temperature in growing season.
470 Specifically, the easternmost part of this ecoregion is characterized by peaty soils (SWC>200
471 mm), leading to root hypoxia, which tends to reduce birch growth (Glenz et al., 2006). These
472 conditions correspond to the ecological niche constraints of *B. pendula*, which is known to
473 thrive less in cooler climates and wetter soils, as evidenced by its distribution range extending
474 further south than north (Atkinson, 1992). However, the uplands ecoregion may become
475 suitable for birch silviculture in the coming decades (Fig. 7), as the growing season will likely
476 lengthen.



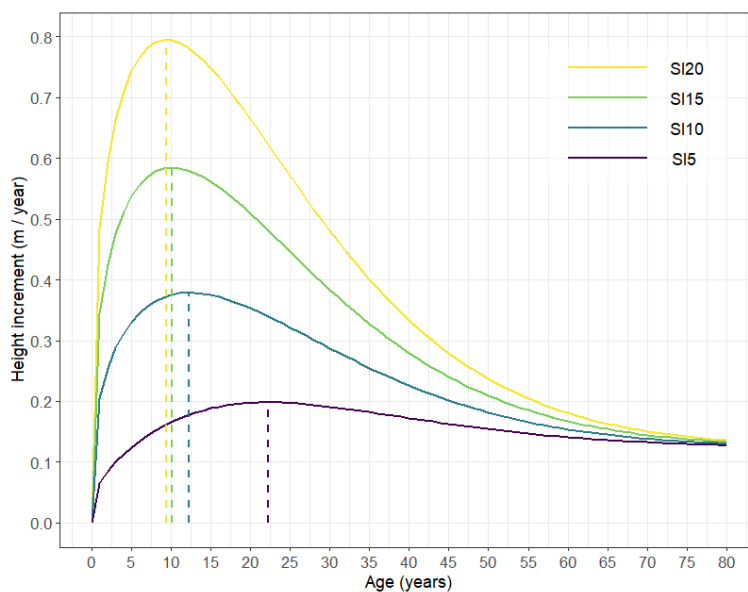
477

478 *Fig. 7: Estimated increase in the site index (SI) of silver birch in southern Belgium due to an*
 479 *increase of 1.5°C in mean annual temperature (compared to the reference period 1961-1990).*
 480 *Predictions outside the range of observed values of site index are displayed in red.*

481 4.3 Applicability of the phytocentric and geocentric models

482 The phytocentric model is valid for pure, even-aged birch stands originating from natural
 483 regeneration, regardless of the birch species. Given the wide range of growth conditions
 484 represented in the sampling, the model is applicable throughout southern Belgium (Figure
 485 S8.2). However, its application in other regions may result in inaccurate productivity estimates
 486 due to local variations in height growth patterns (Fig. 6). The site index can be reliably estimated
 487 for stands aged between 20 and 60 years. In the case of stands younger than 20 years, the
 488 estimation of the site index should be considered with caution due to the high level of
 489 uncertainty in the SI estimation error (Figure S8.1). Due to the limited number of observations

490 beyond 60 years, the interpretation of the site index for older stands should be approached with
491 caution. The proposed model is calibrated at the tree level rather than the stand level. Unlike
492 stand-level models, it does not account for silvicultural interventions that can lead to dominant
493 height reaching a horizontal asymptote more quickly or even decreasing. Nonetheless, if the
494 model is applied in contexts where the dominant tree cohort remains relatively stable, the
495 differences between tree- and stand-level predictions should be minimal. Stability in this cohort
496 can be maintained through target trees silviculture, which focuses management efforts on a
497 limited number of dominant trees, as recommended for birch (Dubois et al., 2021). Peak height
498 growth occurs around 10 years of age (Fig. 8), emphasizing the importance of early
499 management to capitalize on birch's growth potential, as recommended for birch silviculture in
500 Western Europe (Dubois et al., 2021).



501

502 *Fig. 8: Height increment curves for each class of productivity (5, 10, 15 and 20 m at 30*
503 *years). Dashed lines indicate the peak height growth.*

504 The geocentric model is intended to guide the management of pure stands of silver birch. It is
505 applicable in southern Belgium (Figure S8.2), except in the west of the lowlands ecoregion and
506 the northwest of the uplands ecoregion, where the lack of data—and consequently the
507 extrapolation beyond the model's calibration climatic range—leads to inaccurate site index
508 estimates (error of 3.2 m; 95% intervals; Figure S6). The model's climatic applicability range
509 is limited to regions with an average annual temperature between 7.5°C and 9.5°C, and its use
510 is not recommended for areas with a soil water content below 50 mm (Fig. 4). However, the
511 temperature increases induced by climate change imply that 70% of the region (Figure S5),
512 mostly corresponding to the lowlands ecoregion, will exceed the model's calibration climatic
513 range by 2070, resulting in SI estimation errors of up to 8.1 m (95% intervals; Figure S7).
514 Nonetheless, predictions remain reliable in the uplands ecoregion (error of 1.2 m; 95%
515 intervals; Figure S7), where an increase in the potential productivity of birch is to be expected,
516 provided that soil water reserves remain sufficient (> 150 mm; Fig. 7).

517 4.4 Study limitations and perspectives

518 Stem analysis is the fastest way to obtain detailed information on tree growth without the need
519 for long-term measurements, as it is the case with permanent sample plots (Raulier *et al.*, 2003).
520 Stem analysis provides insight into past growth dynamics across multiple variables at the tree
521 level, making it a valuable tool for understanding historical growth trends (Salas-Eljatib, 2021).
522 However, this method has certain limitations. A key issue is the assumption that the sampled
523 trees were dominant throughout their lives, which is not guaranteed. Consequently, stem
524 analysis may overestimate dominant height growth (Raulier *et al.*, 2003), and dominant trees at
525 the time of sampling may have experienced periods of lower dominance at younger ages
526 (Magnussen and Penner, 1996). However, silver birch maintains vigorous growth and vitality
527 only when growing as a dominant tree (Hynynen *et al.*, 2010), as this shade-intolerant species
528 is highly sensitive to competition for light, especially from close neighbours (Vanhellemont *et*

529 *al.*, 2016). This is particularly relevant in naturally regenerated stands, being the most common
530 type of birch stands in Belgium, where intraspecific competition is intense (Dubois *et al.*, 2020).
531 Given the ecological characteristics of birch, the dominance assumption seems reasonable, but
532 this should be verified by comparing our results with permanent sample plots data.

533 The method proposed by Goelz and Burk (1992), based on the relative error of height
534 predictions at different ages, led to the selection of a reference age of 30 years for silver birch.
535 This choice was influenced by several considerations, including the preference for a reference
536 age younger than the minimum rotation age set at 50 years in a target tree silvicultural approach
537 as proposed by Dubois *et al.* (2021). However, the choice of reference age using the relative
538 error method is highly dependent on the age range covered by the dataset. In this study, the
539 number of observations decreases significantly after 30 years, making it difficult to select a
540 reference age closer to the minimum rotation age. While a reference age that is too young may
541 lead to errors in site index estimation, Diéguez-Aranda *et al.* (2005) emphasised that, from a
542 practical perspective, a younger reference age allows earlier decisions on silvicultural
543 treatments. In general, a reference age of 50 years is often used for birch. However, based on
544 the relative error method, Diéguez-Aranda *et al.* (2006) proposed a reference age of 20 years
545 for downy birch in northwestern Spain. In our case, height growth decreases sharply from
546 around 30 years, making this age a suitable compromise for defining the site index of silver
547 birch.

548 The two birch species were not considered separately to produce the dominant height growth
549 model. However, the height growth curve of the two species might differ. Some authors have
550 put forward the hypothesis of a possible hybridization between *B.pendula* and *B.pubescens*
551 despite a different ploidy (Tsuda *et al.*, 2017; Vetchinnikova and Titov, 2023), silver birch being
552 diploid ($2n=28$) and downy birch being tetraploid ($2n=56$; Palmé *et al.*, 2004, 2003). Comparing
553 the growth patterns of these two species and hybrids with precise genetic identification could

554 reveal whether separate growth models are necessary to enhance site index estimates, as
555 demonstrated by Johansson (2013) for hybrid aspen.

556 Due to the absence of past silvicultural management and the lack of interest for birch, the
557 sampling was limited. In this study, the geocentric method-based model considered a limited
558 climatic range. However, to account for climate change, the sampling area should be expanded
559 to encompass a broader climatic range, which will allow for more reliable predictions (Aertsen
560 *et al.*, 2012).

561 The geocentric model relies on spatial data. Although easily accessible, cartographic data limits
562 the choice of variables and may be imprecise, leading to a small percentage of the explained
563 variability (Pinno *et al.*, 2009). In our study, the use of spatial data led to a relatively high
564 percentage of variability being explained (R^2 adj=0.50; Table C1) and allowed birch potential
565 productivity to be mapped at a large scale, providing forest managers with recommendations at
566 a regional scale. In southern Belgium (17,000 km²), environmental conditions—such as climate,
567 topography, and soil—have been well-studied over time. Soil properties were mapped between
568 1950 and 1990 and subsequently digitized (Legrain *et al.*, 2014). At a smaller scale, field data
569 could be obtained in order to quantify the loss of precision associated with the use of spatial
570 data and the eventual need of additional calibration procedures.

571 In the geocentric approach, we used climate data averaged over a 30-year period. This does not
572 allow to take into account the impact of short-term extreme climatic events, such as droughts,
573 which can be detrimental for growth. A dendroecological analysis is needed to assess the impact
574 of such extreme climatic events on birch growth (Fritts and Swetnam, 1989).

575 **Conclusion**

576 Using a phytocentric approach, we developed dominant height growth curves for birch based
577 on stem analyses of 68 trees from 40 stands covering most of the birch range geographic
578 locations and site conditions in southern Belgium. Among the models tested, the Duplat and
579 Tran-Ha I model best predicted the dominant height growth. This model can now be used as a
580 practical tool for forest owners and managers to assess the potential productivity of any even-
581 aged birch stand.

582 We used a geocentric approach to investigate the relationship between the site index of silver
583 birch and biophysical factors. The main factors influencing the site index were the mean annual
584 temperature and the maximal soil water content. The positive effect of higher temperature was
585 limited by soil water content. These results suggest that, in the context of a warmer climate,
586 birch productivity could increase in the uplands where soil water availability is high but
587 decrease in the lowlands on dry soils. The predictive maps identify optimal areas for birch
588 silviculture and regions where its productivity may increase, providing crucial insights for
589 guiding forest management strategies.

590 **Acknowledgements**

591 This study was partly funded by the Plan quinquennal de recherches forestières of the Service
592 Public de Wallonie (forest administration) and by the FNRS (Research Fellow grant awarded
593 to L.Zeoli). We are very grateful to the technicians at the GRF unit (ULiège – Gembloux Agro-
594 Bio Tech), M. Borremans and M. Lemaigre for their valuable work in the field. We would like
595 to thank M. Daffe for his contribution to the preparation of the stem sections, from sanding to
596 counting the ring-widths. Our gratitude also goes to Jérôme Perin and Jonathan Lisein for their
597 valuable advice regarding the methodology and the discussion of the results.

598 **5 Bibliography**

- 599 Aertsen, W., Kint, V., Muys, B., Van Orshoven, J., 2012. Effects of scale and scaling in
600 predictive modelling of forest site productivity. *Environ. Model. Softw.* 31, 19–27.
601 <https://doi.org/10.1016/j.envsoft.2011.11.012>
- 602 Albert, M., Schmidt, M., 2010. Climate-sensitive modelling of site-productivity relationships
603 for Norway spruce (*Picea abies* (L.) Karst.) and common beech (*Fagus sylvatica* L.).
604 *For. Ecol. Manag.* 259, 739–749. <https://doi.org/10.1016/j.foreco.2009.04.039>
- 605 Álvarez-Álvarez, P., Khouri, E.A., Cámara-Obregón, A., Castedo-Dorado, F., Barrio-Anta, M.,
606 2011. Effects of foliar nutrients and environmental factors on site productivity in *Pinus*
607 *pinaster* Ait. stands in Asturias (NW Spain). *Ann. For. Sci.* 68, 497–509.
608 <https://doi.org/10.1007/s13595-011-0047-5>
- 609 Arthur, G., Jonathan, L., Juliette, C., Nicolas, L., Christian, P., Hugues, C., 2024. Spatial and
610 remote sensing monitoring shows the end of the bark beetle outbreak on Belgian and
611 north-eastern France Norway spruce (*Picea abies*) stands. *Environ. Monit. Assess.* 196,
612 226. <https://doi.org/10.1007/s10661-024-12372-0>
- 613 Atkinson, M.D., 1992. *Betula Pendula* Roth (*B. Verrucosa* Ehrh.) and *B. Pubescens* Ehrh. *J.*
614 *Ecol.* 80, 34. <https://doi.org/10.2307/2260870>
- 615 Aurore, F., Annabel, P., Grégory, M., Arnaud, M., 2024. Fast height growth is key to non-native
616 conifers invasiveness in temperate forests. *Biol. Invasions* 26, 857–874.
617 <https://doi.org/10.1007/s10530-023-03214-0>
- 618 Biber, P., Felton, A., Nieuwenhuis, M., Lindbladh, M., Black, K., Bahýl', J., Bingöl, Ö., Borges,
619 J.G., Botequim, B., Brukas, V., Bugalho, M.N., Corradini, G., Eriksson, L.O., Forsell,
620 N., Hengeveld, G.M., Hoogstra-Klein, M.A., Kadioğulları, A.İ., Karahalil, U., Lodin,
621 I., Lundholm, A., Makrickienė, E., Masiero, M., Mozgeris, G., Pivoriūnas, N.,
622 Poschenrieder, W., Pretzsch, H., Sedmák, R., Tuček, J., 2020. Forest Biodiversity,
623 Carbon Sequestration, and Wood Production: Modeling Synergies and Trade-Offs for
624 Ten Forest Landscapes Across Europe. *Front. Ecol. Evol.* 8, 547696.
625 <https://doi.org/10.3389/fevo.2020.547696>
- 626 Bolte, A., Ammer, C., Löf, M., Madsen, P., Nabuurs, G.-J., Schall, P., Spathelf, P., Rock, J.,
627 2009. Adaptive forest management in central Europe: Climate change impacts,
628 strategies and integrative concept. *Scand. J. For. Res.* 24, 473–482.
629 <https://doi.org/10.1080/02827580903418224>
- 630 Bontemps, J.-D., Hervé, J.-C., Dhôte, J.-F., 2009. Long-Term Changes in Forest Productivity:
631 A Consistent Assessment in Even-Aged Stands. *For. Sci.* 55, 549–564.
632 <https://doi.org/10.1093/forestscience/55.6.549>
- 633 Bormann, B.T., Darbyshire, R.L., Homann, P.S., Morrisette, B.A., Little, S.N., 2015.
634 Managing early succession for biodiversity and long-term productivity of conifer forests
635 in southwestern Oregon. *For. Ecol. Manag.* 340, 114–125.
636 <https://doi.org/10.1016/j.foreco.2014.12.016>
- 637 Brandl, S., Mette, T., Falk, W., Vallet, P., Rötzer, T., Pretzsch, H., 2018. Static site indices from
638 different national forest inventories: harmonization and prediction from site conditions.
639 *Ann. For. Sci.* 75, 56. <https://doi.org/10.1007/s13595-018-0737-3>

- 640 Brockerhoff, E.G., Barbaro, L., Castagneyrol, B., Forrester, D.I., Gardiner, B., González-
641 Olabarria, J.R., Lyver, P.O., Meurisse, N., Oxbrough, A., Taki, H., Thompson, I.D., van
642 der Plas, F., Jactel, H., 2017. Forest biodiversity, ecosystem functioning and the
643 provision of ecosystem services. *Biodivers. Conserv.* 26, 3005–3035.
644 <https://doi.org/10.1007/s10531-017-1453-2>
- 645 Büntgen, U., Urban, O., Krusic, P.J., Rybníček, M., Kolář, T., Kyncl, T., Ač, A., Koňasová, E.,
646 Čáslavský, J., Esper, J., Wagner, S., Saurer, M., Tegel, W., Dobrovlný, P., Cherubini,
647 P., Reinig, F., Trnka, M., 2021. Recent European drought extremes beyond Common
648 Era background variability. *Nat. Geosci.* 14, 190–196. <https://doi.org/10.1038/s41561-021-00698-0>
- 650 Campioli, M., Vincke, C., Jonard, M., Kint, V., Demarée, G., Ponette, Q., 2012. Current status
651 and predicted impact of climate change on forest production and biogeochemistry in the
652 temperate oceanic European zone: review and prospects for Belgium as a case study. *J.*
653 *For. Res.* 17, 1–18. <https://doi.org/10.1007/s10310-011-0255-8>
- 654 Carmean, W.H., 1996. Site-quality evaluation, site-quality maintenance, and site-specific
655 management for forest land in northwest Ontario. Ontario Ministry of Natural
656 Resources, Northwest Science and Technology, Thunder Bay.
- 657 Claessens, H., Pauwels, D., Thibaut, A., Rondeux, J., 1999. Site index curves and autecology
658 of ash, sycamore and cherry in Wallonia (Southern Belgium). *Forestry* 72, 171–182.
659 <https://doi.org/10.1093/forestry/72.3.171>
- 660 Combaud, M., Cordonnier, T., Dupire, S., Vallet, P., 2024. Climate change altered the dynamics
661 of stand dominant height in forests during the past century – Analysis of 20 European
662 tree species. *For. Ecol. Manag.* 553, 121601.
663 <https://doi.org/10.1016/j.foreco.2023.121601>
- 664 Diéguez-Aranda, U., Burkhart, H.E., Rodríguez-Soalleiro, R., 2005. Modeling dominant height
665 growth of radiata pine (*Pinus radiata* D. Don) plantations in north-western Spain. *For.*
666 *Ecol. Manag.* 215, 271–284. <https://doi.org/10.1016/j.foreco.2005.05.015>
- 667 Diéguez-Aranda, U., Grandas-Arias, J., Álvarez-González, J., Gadow, K., 2006. Site quality
668 curves for birch stands in north-western Spain. *Silva Fenn.* 40.
669 <https://doi.org/10.14214/sf.319>
- 670 Dimitrova, A., Csilléry, K., Klisz, M., Lévesque, M., Heinrichs, S., Cailleret, M., Andivia, E.,
671 Madsen, P., Böhenius, H., Cvjetkovic, B., De Cuyper, B., de Dato, G., Ferus, P., Heinze,
672 B., Ivetić, V., Köbölkuti, Z., Lazarević, J., Lazdina, D., Maaten, T., Makovskis, K.,
673 Milovanović, J., Monteiro, A.T., Nonić, M., Place, S., Puchalka, R., Montagnoli, A.,
674 2022. Risks, benefits, and knowledge gaps of non-native tree species in Europe. *Front.*
675 *Ecol. Evol.* 10, 908464. <https://doi.org/10.3389/fevo.2022.908464>
- 676 Donis, J., 2022. Algoritmu izstrāde mežsaimniecības plānošanai [Development of algorithms
677 for forestry planning] (Overview of the study 2022 No. 5- 5.9.1_007h_101_21_71),
678 PĀRSKATS PAR PĒTĪJUMA 2022. GADA REZULTĀTIEM [Annual results].
679 Latvian State Forest Research Institute (SILAVA), Salaspils, Latvia.
- 680 Dubois, H., Claessens, H., Ligot, G., 2021. Towards Silviculture Guidelines to Produce Large-
681 Sized Silver Birch (*Betula pendula* Roth) Logs in Western Europe. *Forests* 12, 599.
682 <https://doi.org/10.3390/f12050599>
- 683 Dubois, H., Verkasalo, E., Claessens, H., 2020. Potential of Birch (*Betula pendula* Roth and *B.*
684 *pubescens* Ehrh.) for Forestry and Forest-Based Industry Sector within the Changing

- 685 Climatic and Socio-Economic Context of Western Europe. *Forests* 11, 336.
686 <https://doi.org/10.3390/f11030336>
- 687 Ellenberg, H., 1996. *Vegetation Mitteleuropas Mit Den Alpen in Ökologischer, Dynamischer*
688 *Und Historischer Sicht*, Stark veränd. u. verb. Aufl. ed. Ulmer, Stuttgart.
- 689 Eriksson, H., Johansson, U., Kiviste, A., 1997. A site-index model for pure and mixed stands
690 of *Betula pendula* and *Betula pubescens* in Sweden. *Scand. J. For. Res.* 12, 149–156.
691 <https://doi.org/10.1080/02827589709355396>
- 692 Felton, A., Gustafsson, L., Roberge, J.-M., Ranius, T., Hjältén, J., Rudolphi, J., Lindbladh, M.,
693 Weslien, J., Rist, L., Brunet, J., Felton, A.M., 2016. How climate change adaptation and
694 mitigation strategies can threaten or enhance the biodiversity of production forests:
695 Insights from Sweden. *Biol. Conserv.* 194, 11–20.
696 <https://doi.org/10.1016/j.biocon.2015.11.030>
- 697 Fontes, L., Bontemps, J.-D., Bugmann, H., Van Oijen, M., Gracia, C., Kramer, K., Lindner, M.,
698 Rötzer, T., Skovsgaard, J.P., 2010. Models for supporting forest management in a
699 changing environment. *For. Syst.* 19, 8–29. <https://doi.org/10.5424/fs/201019S-9315>
- 700 Fritts, H.C., Swetnam, T.W., 1989. Dendroecology: a tool for evaluating variations in past and
701 present forest environments, in: *Advances in Ecological Research*. Elsevier, pp. 111–
702 188. [https://doi.org/10.1016/S0065-2504\(08\)60158-0](https://doi.org/10.1016/S0065-2504(08)60158-0)
- 703 Fuchs, S., Schuldt, B., Leuschner, C., 2021. Identification of drought-tolerant tree species
704 through climate sensitivity analysis of radial growth in Central European mixed
705 broadleaf forests. *For. Ecol. Manag.* 494, 119287.
706 <https://doi.org/10.1016/j.foreco.2021.119287>
- 707 George, J. -P., Bürkner, P. -C., Sanders, T.G.M., Neumann, M., Cammalleri, C., Vogt, J.V.,
708 Lang, M., 2022. Long-term forest monitoring reveals constant mortality rise in
709 European forests. *Plant Biol.* 24, 1108–1119. <https://doi.org/10.1111/plb.13469>
- 710 Glenz, C., Schlaepfer, R., Iorgulescu, I., Kienast, F., 2006. Flooding tolerance of Central
711 European tree and shrub species. *For. Ecol. Manag.* 235, 1–13.
712 <https://doi.org/10.1016/j.foreco.2006.05.065>
- 713 Goelz, J.C.G., Burk, T.E., 1992. Development of a well-behaved site index equation: jack pine
714 in north central Ontario. *Can. J. For. Res.* 22, 776–784. <https://doi.org/10.1139/x92-106>
- 715 Gustavsen, H.G., Mielikäinen, K., 1984. Luontaisesti syntyneiden koivikoiden
716 kasvupaikkaluokittelu valtapituuden avulla [Site index curves for natural birch stands
717 in Finland]. *Folia For.* 597, 1–23.
- 718 Hein, S., Winterhalter, D., Wilhelm, G.J., Kohnle, U., 2009. Wertholzproduktion mit der
719 Sandbirke (*Betula pendula* Roth): waldbauliche Möglichkeiten und Grenzen. *Allg.*
720 *Forst Jagdztg.* 180, 206–219.
- 721 Hemery, G.E., Clark, J.R., Aldinger, E., Claessens, H., Malvoti, M.E., O’connor, E.,
722 Raftoyannis, Y., Savill, P.S., Brus, R., 2010. Growing scattered broadleaved tree species
723 in Europe in a changing climate: a review of risks and opportunities. *Forestry* 83, 65–
724 81. <https://doi.org/10.1093/forestry/cpp034>
- 725 Hlásny, T., König, L., Krokene, P., Lindner, M., Montagné-Huck, C., Müller, J., Qin, H., Raffa,
726 K.F., Schelhaas, M.-J., Svoboda, M., Viiri, H., Seidl, R., 2021. Bark Beetle Outbreaks

- 727 in Europe: State of Knowledge and Ways Forward for Management. *Curr. For. Rep.* 7,
728 138–165. <https://doi.org/10.1007/s40725-021-00142-x>
- 729 Hynynen, J., Niemisto, P., Vihera-Aarnio, A., Brunner, A., Hein, S., Velling, P., 2010.
730 Silviculture of birch (*Betula pendula* Roth and *Betula pubescens* Ehrh.) in northern
731 Europe. *Forestry* 83, 103–119. <https://doi.org/10.1093/forestry/cpp035>
- 732 Johansson, T., 2013. A site dependent top height growth model for hybrid aspen. *J. For. Res.*
733 24, 691–698. <https://doi.org/10.1007/s11676-013-0365-6>
- 734 Jonczak, J., Jankiewicz, U., Kondras, M., Kruczkowska, B., Oktaba, L., Oktaba, J., Olejniczak,
735 I., Pawłowicz, E., Polláková, N., Raab, T., Regulska, E., Słowińska, S., Sut-Lohmann,
736 M., 2020. The influence of birch trees (*Betula* spp.) on soil environment – A review.
737 *For. Ecol. Manag.* 477, 118486. <https://doi.org/10.1016/j.foreco.2020.118486>
- 738 Journée, M., Ingels, R., Bertrand, C., 2019. Overview and validation of observational gridded
739 data products for Belgium, in: EMS Annual Meeting Abstracts. Lyngby Campus, pp.
740 2019–2099.
- 741 Karlsson, A., Albrektson, A., Sonesson, J., 1997. Site index and productivity of artificially
742 regenerated *Betula pendula* and *Betula pubescens* stands on former farmland in southern
743 and central Sweden. *Scand. J. For. Res.* 12, 256–263.
744 <https://doi.org/10.1080/02827589709355408>
- 745 Kiviste, A., Tarmu, T., Padari, A., Laarman, D., 2022. Modelling dominant height development
746 on estonian forest permanent plot data, in: SNS Growth and Yield Nordic Biannual
747 Conference. Presented at the Local solutions for regional and global forest management
748 challenges, Rīga, Latvia, pp. 8–9.
- 749 Koch, O., de Avila, A.L., Heinen, H., Albrecht, A.T., 2022. Retreat of Major European Tree
750 Species Distribution under Climate Change—Minor Natives to the Rescue?
751 *Sustainability* 14, 5213. <https://doi.org/10.3390/su14095213>
- 752 Kunz, J., Löffler, G., Bauhus, J., 2018. Minor European broadleaved tree species are more
753 drought-tolerant than *Fagus sylvatica* but not more tolerant than *Quercus petraea*. *For.*
754 *Ecol. Manag.* 414, 15–27. <https://doi.org/10.1016/j.foreco.2018.02.016>
- 755 Latte, N., Taverniers, P., de Jaegere, T., Claessens, H., 2020. Dendroecological assessment of
756 climate resilience of the rare and scattered forest tree species *Tilia cordata* Mill. in
757 northwestern Europe. *For. Int. J. For. Res.* 93, 675–684.
758 <https://doi.org/10.1093/forestry/cpaa011>
- 759 Le Goff, N., Garros, A., Canta, R., Fertin, D., 1982. Productivité du frêne en région Nord-
760 Picardie A. - Courbes de croissance en hauteur. *Ann. Sci. For.* 39, 259–288.
- 761 Lee, D., Siipilehto, J., Miina, J., Niemistö, P., Haapanen, M., Hynynen, J., Huuskonen, S., 2024.
762 Site index and stand characteristic models for silver birch plantations in southern and
763 central Finland. *For. Ecol. Manag.* 563, 121998.
764 <https://doi.org/10.1016/j.foreco.2024.121998>
- 765 Legrain, X., Bock, L., Colinet, G., 2014. Suitability of the soil map and legacy data in Wallonia
766 (BE) to support the GSM initiative, in: Arrouays, D., McKenzie, N., Hempel, J., De
767 Forges, A., McBratney, A. (Eds.), *GlobalSoilMap*. CRC Press, pp. 99–102.
768 <https://doi.org/10.1201/b16500-21>

- 769 Leuschner, C., Fuchs, S., Wedde, P., R  ther, E., Schuldt, B., 2024. A multi-criteria drought
770 resistance assessment of temperate *Acer*, *Carpinus*, *Fraxinus*, *Quercus*, and *Tilia*
771 species. *Perspect. Plant Ecol. Evol. Syst.* 62, 125777.
772 <https://doi.org/10.1016/j.ppees.2023.125777>
- 773 Lindner, M., Lasch, P., Erhard, M., 2000. Alternative forest management strategies under
774 climatic change – prospects for gap model applications in risk analyses. *Silva Fenn.* 34.
775 <https://doi.org/10.14214/sf.634>
- 776 Lindner, M., Maroschek, M., Netherer, S., Kremer, A., Barbati, A., Garcia-Gonzalo, J., Seidl,
777 R., Delzon, S., Corona, P., Kolstr  m, M., Lexer, M.J., Marchetti, M., 2010. Climate
778 change impacts, adaptive capacity, and vulnerability of European forest ecosystems.
779 *For. Ecol. Manag.* 259, 698–709. <https://doi.org/10.1016/j.foreco.2009.09.023>
- 780 Lisein, J., Fayolle, A., Legrain, A., Pr  vot, C., Claessens, H., 2022. Prediction of forest nutrient
781 and moisture regimes from understory vegetation with random forest classification
782 models. *Ecol. Indic.* 144, 109446. <https://doi.org/10.1016/j.ecolind.2022.109446>
- 783 Liziniewicz, M., Barbeito, I., Zvirgzdins, A., Stener, L.-G., Niemist  , P., Fahlvik, N.,
784 Johansson, U., Karlsson, B., Nilsson, U., 2022. Production of genetically improved
785 silver birch plantations in southern and central Sweden. *Silva Fenn.* 56.
786 <https://doi.org/10.14214/sf.10512>
- 787 Luostarinen, K., Verkasalo, E., 2000. Birch as sawn timber and in mechanical further
788 processing in Finland: a literature study, *Silva Fennica monographs*. The Finnish Soc. of
789 Forest Science [u.a.], Joensuu.
- 790 Magnussen, S., Penner, M., 1996. Recovering time trends in dominant height from stem
791 analysis. *Can. J. For. Res.* 26, 9–22. <https://doi.org/10.1139/x26-002>
- 792 Martinez del Castillo, E., Zang, C.S., Buras, A., Hacket-Pain, A., Esper, J., Serrano-Notivoli,
793 R., Hartl, C., Weigel, R., Klesse, S., Resco de Dios, V., Scharnweber, T., Dorado-Li  n,
794 I., van der Maaten-Theunissen, M., van der Maaten, E., Jump, A., Mikac, S., Banzragch,
795 B.-E., Beck, W., Cavin, L., Claessens, H.,   ada, V.,   ufar, K., Dulamsuren, C., Gri  ar,
796 J., Gil-Pelegr  n, E., Janda, P., Kazimirovic, M., Kreyling, J., Latte, N., Leuschner, C.,
797 Longares, L.A., Menzel, A., Merela, M., Motta, R., Muffler, L., Nola, P., Petritan, A.M.,
798 Petritan, I.C., Prisl  n, P., Rubio-Cuadrado,   ., Rydval, M., Staji  , B., Svoboda, M.,
799 Toromani, E., Trotsiuk, V., Wilmking, M., Zlatanov, T., de Luis, M., 2022. Climate-
800 change-driven growth decline of European beech forests. *Commun. Biol.* 5, 163.
801 <https://doi.org/10.1038/s42003-022-03107-3>
- 802 Matisons, R., Jansone, D., Elferts, D., Schneck, V., Kowalczyk, J., Wojda, T., Jansons,   .,
803 2022. Silver birch shows nonlinear responses to moisture availability and temperature
804 in the eastern Baltic Sea region. *Dendrochronologia* 76, 126003.
805 <https://doi.org/10.1016/j.dendro.2022.126003>
- 806 Messier, C., Bauhus, J., Sousa-Silva, R., Auge, H., Baeten, L., Barsoum, N., Bruelheide, H.,
807 Caldwell, B., Cavender-Bares, J., Dhiedt, E., Eisenhauer, N., Ganade, G., Gravel, D.,
808 Guillemot, J., Hall, J.S., Hector, A., H  rault, B., Jactel, H., Koricheva, J., Kreft, H.,
809 Mereu, S., Muys, B., Nock, C.A., Paquette, A., Parker, J.D., Perring, M.P., Ponette, Q.,
810 Potvin, C., Reich, P.B., Scherer-Lorenzen, M., Schnabel, F., Verheyen, K., Weih, M.,
811 Wollni, M., Zemp, D.C., 2022. For the sake of resilience and multifunctionality, let’s
812 diversify planted forests! *Conserv. Lett.* 15, e12829. <https://doi.org/10.1111/conl.12829>

- 813 Millar, C.I., Stephenson, N.L., Stephens, S.L., 2007. Climate change and forests of the future:
814 managing in the face of uncertainty. *Ecol. Appl.* 17, 2145–2151.
815 <https://doi.org/10.1890/06-1715.1>
- 816 Mueller, J.M., Hellmann, J.J., 2008. An Assessment of Invasion Risk from Assisted Migration.
817 *Conserv. Biol.* 22, 562–567. <https://doi.org/10.1111/j.1523-1739.2008.00952.x>
- 818 Nakatsu, R.T., 2021. An Evaluation of Four Resampling Methods Used in Machine Learning
819 Classification. *IEEE Intell. Syst.* 36, 51–57. <https://doi.org/10.1109/MIS.2020.2978066>
- 820 Oikarinen, M., 1983. Etelä-Suomen viljeltyjen rauduskoivikoiden kasvatusmallit. [Growth and
821 yield models for silver birch (*Betula pendula*) plantations in southern Finland].
822 *Commun. Inst. For. Fenn* 113, 75.
- 823 Palmé, A.E., Su, Q., Palsson, S., Lascoux, M., 2004. Extensive sharing of chloroplast
824 haplotypes among European birches indicates hybridization among *Betula pendula*, *B.*
825 *pubescens* and *B. nana*. *Mol. Ecol.* 13, 167–178. <https://doi.org/10.1046/j.1365-294X.2003.02034.x>
- 827 Palmé, A.E., Su, Q., Rautenberg, A., Manni, F., Lascoux, M., 2003. Postglacial recolonization
828 and cpDNA variation of silver birch, *Betula pendula*. *Mol. Ecol.* 12, 201–212.
829 <https://doi.org/10.1046/j.1365-294X.2003.01724.x>
- 830 Parresol, B.R., Scott, D.A., Zarnoch, S.J., Edwards, L.A., Blake, J.I., 2017. Modeling forest site
831 productivity using mapped geospatial attributes within a South Carolina Landscape,
832 USA. *For. Ecol. Manag.* 406, 196–207. <https://doi.org/10.1016/j.foreco.2017.10.006>
- 833 Patacca, M., Lindner, M., Lucas-Borja, M.E., Cordonnier, T., Fidej, G., Gardiner, B., Hauf, Y.,
834 Jasinevičius, G., Labonne, S., Linkevičius, E., Mahnken, M., Milanovic, S., Nabuurs,
835 G., Nagel, T.A., Nikinmaa, L., Panyatov, M., Bercak, R., Seidl, R., Ostrogović Sever,
836 M.Z., Socha, J., Thom, D., Vuletic, D., Zudin, S., Schelhaas, M., 2023. Significant
837 increase in natural disturbance impacts on European forests since 1950. *Glob. Change*
838 *Biol.* 29, 1359–1376. <https://doi.org/10.1111/gcb.16531>
- 839 Pau, M., Gauthier, S., Chavardès, R.D., Girardin, M.P., Marchand, W., Bergeron, Y., 2022. Site
840 index as a predictor of the effect of climate warming on boreal tree growth. *Glob.*
841 *Change Biol.* 28, 1903–1918. <https://doi.org/10.1111/gcb.16030>
- 842 Pebesma, E., Bivand, R., 2023. *Spatial Data Science: With Applications in R*, 1st ed. Chapman
843 and Hall/CRC, New York. <https://doi.org/10.1201/9780429459016>
- 844 Perala, D.A., Alm, A.A., 1990. Reproductive ecology of birch: A review. *For. Ecol. Manag.* 32,
845 1–38. [https://doi.org/10.1016/0378-1127\(90\)90104-J](https://doi.org/10.1016/0378-1127(90)90104-J)
- 846 Perin, J., Hébert, J., Brostaux, Y., Lejeune, P., Claessens, H., 2013. Modelling the top-height
847 growth and site index of Norway spruce in Southern Belgium. *For. Ecol. Manag.* 298,
848 62–70. <https://doi.org/10.1016/j.foreco.2013.03.009>
- 849 Pinheiro, J., Bates, D., R Core Team, 2024. *nlme: Linear and Nonlinear Mixed Effects Models*.
- 850 Pinno, B.D., Paré, D., Guindon, L., Bélanger, N., 2009. Predicting productivity of trembling
851 aspen in the Boreal Shield ecozone of Quebec using different sources of soil and site
852 information. *For. Ecol. Manag.* 257, 782–789.
853 <https://doi.org/10.1016/j.foreco.2008.09.058>

- 854 Raulier, F., Lambert, M.-C., Pothier, D., Ung, C.-H., 2003. Impact of dominant tree dynamics
855 on site index curves. *For. Ecol. Manag.* 184, 65–78. <https://doi.org/10.1016/S0378->
856 1127(03)00149-X
- 857 Ridremont, F., Lejeune, P., Claessens, H., 2011. Pragmatic assessment of the water reserve of
858 the forest sites and mapping at the regional scale (Wallonia, Belgium). *Méthode*
859 *pragmatique d'évaluation de la réserve en eau des stations forestières et cartographie à*
860 *l'échelle régionale (Wallonie, Belgique).* *Biotechnol. Agron. Soc. Environ.* 15, 727–
861 741.
- 862 Salas-Eljatib, C., 2021. A new algorithm for reconstructing tree height growth with stem
863 analysis data. *Methods Ecol. Evol.* 12, 2008–2016. <https://doi.org/10.1111/2041->
864 210X.13616
- 865 Schuldt, B., Buras, A., Arend, M., Vitasse, Y., Beierkuhnlein, C., Damm, A., Gharun, M.,
866 Grams, T.E.E., Hauck, M., Hajek, P., Hartmann, H., Hiltbrunner, E., Hoch, G.,
867 Holloway-Phillips, M., Körner, C., Larysch, E., Lübbe, T., Nelson, D.B., Rammig, A.,
868 Rigling, A., Rose, L., Ruehr, N.K., Schumann, K., Weiser, F., Werner, C., Wohlgemuth,
869 T., Zang, C.S., Kahmen, A., 2020. A first assessment of the impact of the extreme 2018
870 summer drought on Central European forests. *Basic Appl. Ecol.* 45, 86–103.
871 <https://doi.org/10.1016/j.baae.2020.04.003>
- 872 Schulzweida, U., Quast, R., 2015. Climate indices with CDO.
- 873 Seynave, I., Gégout, J., Hervé, J., Dhôte, J., 2008. Is the spatial distribution of European beech
874 (*Fagus sylvatica* L.) limited by its potential height growth? *J. Biogeogr.* 35, 1851–1862.
875 <https://doi.org/10.1111/j.1365-2699.2008.01930.x>
- 876 Skovsgaard, J.P., Vanclay, J.K., 2008. Forest site productivity: a review of the evolution of
877 dendrometric concepts for even-aged stands. *Forestry* 81, 13–31.
878 <https://doi.org/10.1093/forestry/cpm041>
- 879 Socha, J., Coops, N., Ochal, W., 2016. Assessment of age bias in site index equations. *IForest*
880 - *Biogeosciences For.* 9, 402–408. <https://doi.org/10.3832/ifor1548-008>
- 881 Spittlehouse, D.L., Stewart, R.B., 2003. Adaptation to climate change in forest management. *J.*
882 *Ecosyst. Manag.* <https://doi.org/10.22230/jem.2004v4n1a254>
- 883 Spurr, S.H., Barnes, B.V., 1973. *Forest ecology*, 2nd ed. ed. Ronald Press Company.
- 884 Stark, H., Nothdurft, A., Block, J., Bauhus, J., 2015. Forest restoration with *Betula* ssp. and
885 *Populus* ssp. nurse crops increases productivity and soil fertility. *For. Ecol. Manag.* 339,
886 57–70. <https://doi.org/10.1016/j.foreco.2014.12.003>
- 887 Swanson, M.E., Franklin, J.F., Beschta, R.L., Crisafulli, C.M., DellaSala, D.A., Hutto, R.L.,
888 Lindenmayer, D.B., Swanson, F.J., 2010. The forgotten stage of forest succession:
889 early-successional ecosystems on forest sites. *Front. Ecol. Environ.* 9, 117–125.
890 <https://doi.org/10.1890/090157>
- 891 Tsuda, Y., Semerikov, V., Sebastiani, F., Vendramin, G.G., Lascoux, M., 2017. Multispecies
892 genetic structure and hybridization in the *Betula* genus across Eurasia. *Mol. Ecol.* 26,
893 589–605. <https://doi.org/10.1111/mec.13885>
- 894 Vanhellemont, M., Van Acker, J., Verheyen, K., 2016. Exploring life growth patterns in birch
895 (*Betula pendula*). *Scand. J. For. Res.* 31, 561–567.
896 <https://doi.org/10.1080/02827581.2016.1141978>

- 897 Vetchinnikova, L.V., Titov, A.F., 2023. Genus *Betula* L.: Species-Specific Population-Genetic
898 Features and Taxonomy Problems. *Biol. Bull. Rev.* 13, S377–S391.
899 <https://doi.org/10.1134/S2079086423090177>
- 900 Walentowski, H., Falk, W., Mette, T., Kunz, J., Bräuning, A., Meinardus, C., Zang, C.,
901 Sutcliffe, L.M.E., Leuschner, C., 2017. Assessing future suitability of tree species under
902 climate change by multiple methods: a case study in southern Germany. *Ann. For. Res.*
903 60. <https://doi.org/10.15287/afr.2016.789>
- 904 Wampach, F., Lisein, J., Cordier, S., Ridremont, F., Claessens, H., 2017. Cartographie de la
905 disponibilité en eau et en éléments nutritifs des stations forestières de Wallonie.
- 906 Wilhelm, G.J., Rieger, H., 2023. QD: une autre gestion de la forêt basée sur la qualité, les cycles
907 naturels et à moindre coût, 2e éd. revue et augmentée. ed. CNPF-IDF, Institut pour le
908 développement forestier “Forêt.nature,” Paris Marche-en-Famenne (Belgique).
- 909 Williams, M.I., Dumroese, R.K., 2013. Preparing for Climate Change: Forestry and Assisted
910 Migration. *J. For.* 111, 287–297. <https://doi.org/10.5849/jof.13-016>
- 911 Wolf, S., Paul-Limoges, E., 2023. Drought and heat reduce forest carbon uptake. *Nat. Commun.*
912 14, 6217. <https://doi.org/10.1038/s41467-023-41854-x>
- 913 Wood, S.N., Pya, N., Säfken, B., 2016. Smoothing Parameter and Model Selection for General
914 Smooth Models. *J. Am. Stat. Assoc.* 111, 1548–1563.
915 <https://doi.org/10.1080/01621459.2016.1180986>
- 916 Zhang, Y., Zhou, X., Guo, J., Sharma, R.P., Zhang, L., Zhou, H., 2022. Modeling the Dominant
917 Height of *Larix principis-rupprechtii* in Northern China—A Study for Guandi
918 Mountain, Shanxi Province. *Forests* 13, 1592. <https://doi.org/10.3390/f13101592>
- 919